



**Effect of steric changes on the isoselectivity of dinuclear
indium catalysts for lactide polymerization**

Journal:	<i>Dalton Transactions</i>
Manuscript ID:	DT-ART-01-2015-000222.R2
Article Type:	Paper
Date Submitted by the Author:	13-Feb-2015
Complete List of Authors:	Mehrkhodavandi, Parisa; University of British Columbia, Chemistry Osten, Kimberley; University of British Columbia, Chemistry Aluthge, Dinesh; University of British Columbia, Chemistry

ARTICLE

Effect of steric changes on the isoselectivity of dinuclear indium catalysts for lactide polymerization

Cite this: DOI: 10.1039/x0xx00000x

K. M. Osten,^a D. C. Aluthge,^a and P. Mehrkhodavandi^aReceived 00th January 2012,
Accepted 00th January 2012

DOI: 10.1039/x0xx00000x

www.rsc.org/

A series of (\pm)- and (*R,R*)- tridentate diamino, *ortho* / *para* disubstituted phenolate proligands H(NNO_R) with various phenolate substituents was synthesized and used to make indium dichloride complexes (NNO_R)InCl₂ via salt metathesis of the deprotonated ligands with indium trichloride. These complexes are dinuclear in the solid state, in contrast to previously reported complexes with *t*-butyl or methyl phenolate substituents. Solution state ¹H and PGSE NMR spectroscopy suggest that a fast exchange between the monomeric and dimeric form of these complexes may exist in solution and is likely influenced by the chirality of the complexes undergoing aggregation. The indium dichloride complexes were utilized to synthesize dinuclear indium ethoxide complexes via salt metathesis with sodium ethoxide. These complexes were active for the polymerization of lactide. *In situ* and bulk polymerization data confirmed differences in the activity and selectivity of these systems based on the phenolate substituents as well as the ligand chirality.

Introduction

The possible commercial and environmental benefits of poly(lactic acid) (PLA) have generated a great deal of interest in improving the properties of this material.¹⁻⁴ In particular, there has been a focus on generating stereoregular PLAs from a mixture of L- and D-lactide, racemic lactide (*rac*-LA), to improve polymer mechanical properties.⁵⁻⁷ Melting point, in particular, is affected strongly by polymer microstructure. Random incorporation of L- and D-lactide forms atactic PLA, which is amorphous, while block copolymers consisting of isotactic L- and D-lactide have melting points greater than 230 °C.⁸ Although organocatalysts have shown some success in controlling polymer tacticity,⁹ the bulk of the work in this area has concentrated on developing metal-based catalysts for the ring opening polymerization (ROP) of *rac*-LA. In particular, there has been a strong interest in group 13 metals.

Two different classes of catalyst have been developed to enforce stereochemical control in the polymerization of *rac*-LA. In the first class, bulky, achiral ligands, which enforce chain-end control, are used as supports for Lewis acidic metals. In particular, various achiral aluminum salen complexes with excellent control of polymer tacticity have been reported.¹⁰⁻²¹ These yield isotactic PLA (*P_m* up to >0.9). In the second class, chiral ligands are used as supports for Lewis acidic metals, enforcing site-control of polymer tacticity. Of this type, chiral aluminum salen complexes show excellent control of polymer tacticity,^{17,18,22-27} although a number of indium-based catalysts with various degrees of isoselectivity have been reported.^{21,28-40}

However, development of a truly isoselective and active catalyst for industrial use remains elusive and a perusal of chiral isoselective systems shows that there is often no straightforward way to attribute catalyst selectivity to ligand substitution patterns.

Our group is interested in the use of Lewis acidic metal catalysts for the polymerization of a variety of cyclic esters to produce biodegradable polymers with commercially relevant properties.⁴¹ In particular, we are interested in the stereoselective polymerization of *rac*-LA to form isotactic stereoblock or stereogradient PLA.^{42,43} To this end, we have reported a family of dinuclear indium alkoxide catalysts with varying degrees of activity and stereoselectivity for the polymerization of racemic lactide.⁴⁴⁻⁴⁹ Our first reported catalyst in this family, parent catalyst [(NNO_{*t*Bu})InCl]₂(μ-Cl)(μ-OEt) (Figure 1), synthesized from the parent dichloride complex (NNO_{*t*Bu})InCl₂, is highly active for the polymerization of racemic lactide but is only modestly isoselective (*P_m* up to 0.62).^{44,48} Our recent efforts to improve this selectivity, by modifications to the terminal amine substituents,⁴⁶ the central amine substituents or the ligand backbone⁵⁰ have not resulted in the isolation of more selective indium catalysts. In each case, the catalyst structure, aggregation pattern, or activity changed with subtle changes to ligand structure.

These challenges highlight the difficulty of predicting stereoselectivity in a given system without a systematic study of ligand substituents. Thus, we wished to explore the role of the phenolate substituents on the activity and stereoselectivity of these types of dinuclear indium complexes in the

polymerization of racemic lactide. We were particularly interested in discerning not only the influence of the steric bulk of these substituents on the stereoselectivity of these complexes but also its influence on their nuclearity and reactivity. This paper will detail the results of these studies.

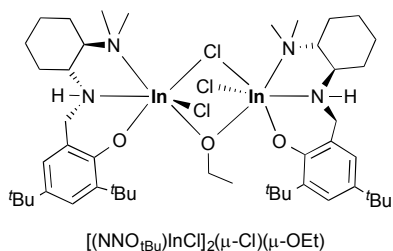
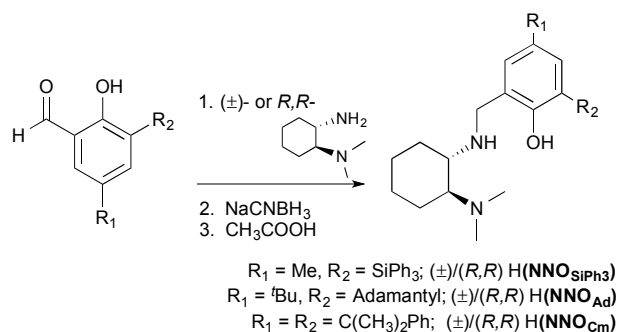


Figure 1. Previously reported dinuclear indium catalyst [(NNO_{tBu})InCl₂]₂(μ-Cl)(μ-OEt) for the polymerization of racemic lactide.

Results and Discussion

Synthesis and characterization of complexes

A family of racemic and enantiopure diaminophenolate proligands with various *ortho*- and *para*-phenolate substituents can be prepared according to previously published procedures (Scheme 1).^{48,51} Condensation of (±)- or (*R,R*)-*N,N*-dimethyl-*trans*-1,2-diaminocyclohexane with the appropriate salicylaldehyde forms the intermediate imines, which can be reduced with NaCNBH₃ to form proligands (±)- and (*R,R*)-H(NNO_{SiPh₃}) (R₁ = Me, R₂ = SiPh₃), H(NNO_{Ad}) (R₁ = ^tBu, R₂ = Adamantyl, Ad) and H(NNO_{Cm}) (R₁ = R₂ = C(CH₃)₂Ph = Cumyl, Cm). The corresponding salicylaldehyde starting materials can be prepared according to published literature procedures.⁵²⁻⁵⁴

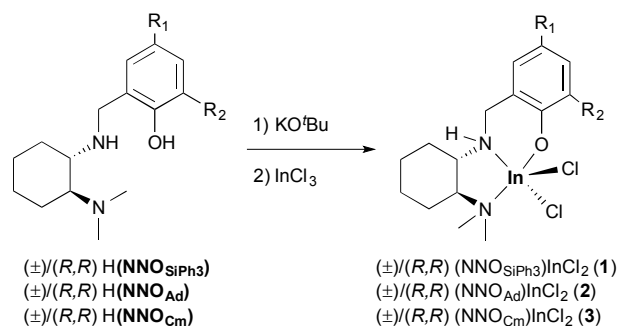


Scheme 1. Synthesis of racemic and enantiopure proligands H(NNO_n) with various phenolate substituents.

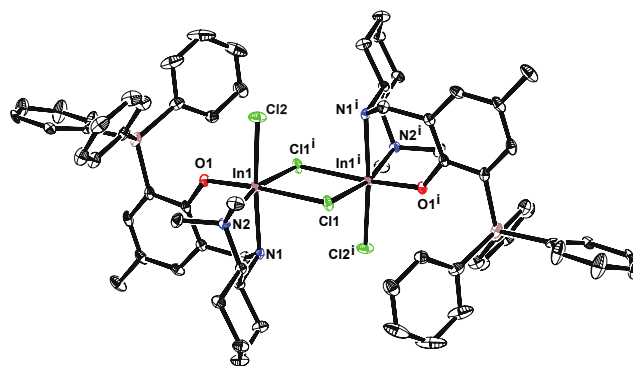
These proligands are both polar and highly soluble in most organic solvents. This complicates the purification process and occasionally results in low yields. In most cases, the compounds can be purified by precipitation and recrystallization from acetonitrile or methanol with the exception of (*R,R*)-H(NNO_{Cm}), which can only be obtained as an oil. The ¹H NMR spectra of the racemic and enantiopure proligands are identical and show the diagnostic N-CH₂-Ar

protons of the ligand backbone as diastereotopic doublets in the 3.8 – 4.1 ppm range for the SiPh₃ and Ad analogues (see SI, Figures S1-2). For the cumyl analogues these protons appear as a broad singlet at 3.81 ppm (Figure S3).

Deprotonation of the proligands (±)- or (*R,R*)-H(NNO_R) with KO^tBu, followed by salt metathesis with InCl₃ affords the dichloride intermediates (±)- and (*R,R*)-(NNO_R)InCl₂ (R₂ = SiPh₃, **1**; Ad, **2**; Cm, **3**) in isolated yields of 30-88 % (Scheme 2).^{44,55} Single crystals of complex (±)-**1** can be obtained at room temperature by slow diffusion of hexane into a saturated solution of the complex in THF and those for (±)-**2** can be obtained from a saturated solution of the complex in toluene. Complex (±)-**3** and all of the enantiopure complexes do not yield single crystals.



Scheme 2. Synthesis of racemic and enantiopure indium dichloride complexes with various phenolate substituents.



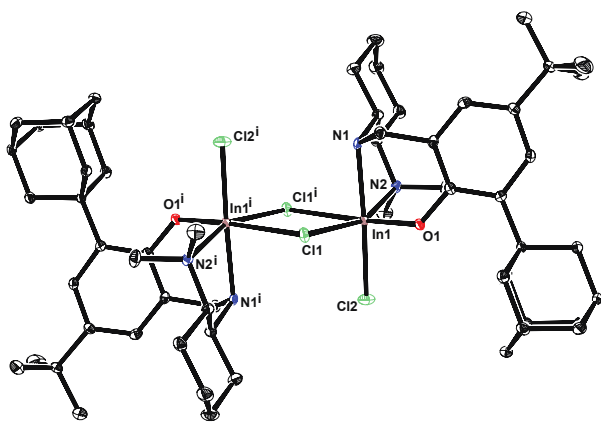


Figure 1. Solid-state molecular structures of complexes (*RR/SS*)-1 (top) and (*RR/SS*)-2 (bottom). Structures are depicted with thermal ellipsoids at 50% probability and solvent and H atoms omitted for clarity. Selected bond lengths (Å) for complex (*RR/SS*)-1: In1-N1 2.2747(12), In1-N2 2.3152(12), In1-Cl1 2.5788(4), In1-Cl1' 2.6160(4), In1-Cl2 2.3938(4), In1-O1 2.0586(10); for complex (*RR/SS*)-2: In1-N1 2.2623(13), In1-N2 2.3281(11), In1-Cl1 2.5622(4), In1-Cl1' 2.6686(4), In1-Cl2 2.4058(4), In1-O1 2.0833(10). Selected bond angles (°) for complex (*RR/SS*)-1: In1-Cl1-In1' 94.901(12), O1-In1-N2 98.88(4), O1-In1-Cl1 168.19(3), O1-In1-Cl1' 86.09(3), N2-In1-Cl1 87.92(3), N2-In1-Cl1' 165.63(3), Cl1-In1-Cl1' 85.099(12), N1-In1-Cl2 173.76(3); for complex (*RR/SS*)-2: In1-Cl1-In1' 99.365(13), O1-In1-N2 104.24(4), O1-In1-Cl1 168.54(3), O1-In1-Cl1' 89.54(3), N2-In1-Cl1 83.63(3), N2-In1-Cl1' 158.55(3), Cl1-In1-Cl1' 80.636(13), N1-In1-Cl2 174.36(3).

The solid-state molecular structures of complexes (\pm)-1 and (\pm)-2 can be determined by single crystal X-ray crystallography (Figure 2). Complexes (\pm)-1 and (\pm)-2 crystallize as heterochiral (*RR/SS*) dimers with an inversion centre and distorted octahedral indium centers bridged by chloride ligands. The two are nearly isostructural and have similar bond lengths and angles (Figure 2; Table S1). The formation of such heterochiral dimers is consistent with previously reported dimeric indium complexes within this ligand family with identical bridging ligands.^{44-46,48,50} However, isolation of dimeric indium dichloride complexes in the solid-state is unusual; all previous solid-state structures of indium halide species in this ligand family have been monomeric.

The ¹H NMR spectra of the (\pm)- and (*R,R*)- analogues of complexes 1-3 are not identical, an indication that aggregation is also occurring in solution to form different species from the racemic and enantiopure complexes (Figure 3). The N-CH₂-Ar protons of the ligand backbone appear as two multiplets at different shifts in the racemic analogues compared to their enantiopure counterparts. In addition, there are small differences in the shifts of the aromatic protons around 7 ppm and the N-CH₃ protons around 2.3 ppm (Figures S4-6). Similar minor differences are present for previously reported (\pm)- and (*R,R*)-(NNO_{*t*Bu})InCl₂ (Figure 3).^{44,48}

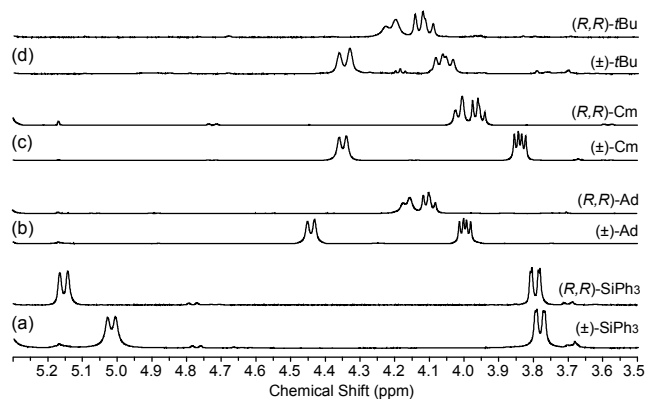


Figure 3. Methylene region of the ¹H NMR spectra (25 °C, CD₂Cl₂, a-c: 600 MHz, d: 400 MHz) of (\pm)- (bottom) and (*R,R*)- (top) analogues of complexes (a) 1, (b) 2 (c) 3 and (d) complex (NNO_{*t*Bu})InCl₂.

The disparity between the solution structures of the racemic and enantiopure dichloride complexes may be due to the chirality of dimeric indium complexes formed with this ligand system. We have reported that heterochiral (*RR/SS*) dimers for bis-ethoxide bridged [(NNO_{*t*Bu})InCl(μ-OEt)]₂ are more thermodynamically stable. A 1:1 mixture of the enantiopure (*RR/RR*) and (*SS/SS*) [(NNO_{*t*Bu})InCl(μ-OEt)]₂ dimers in solution forms the heterochiral species.⁴⁸ Assuming a similar stability of heterochiral dimers in these dichloride complexes, we can hypothesize that if these complexes dimerize in solution, similarly to their solid-state structures, the racemic complexes will form heterochiral dimers whereas the enantiopure complexes will necessarily form homochiral dimers or may remain mononuclear, thus resulting in the disparity between the two spectra.

It is likely that a fast equilibrium between the monomeric and dimeric forms of these complexes exists in solution, as was previously proposed for analogous dimeric indium alkoxide complexes within this ligand family.⁴⁸ As the presence of two sets of peaks in the ¹H NMR spectra of these complexes is not observed at room temperature (see Figure 3 and Figures S4-6) we can assume fast exchange is taking place between the monomeric and dimeric indium chloride species and therefore the chemical shifts would represent an average of the shifts of the two species present in solution. Qualitatively, this is corroborated by the relative broadness of the peaks in the spectra of these compounds (Figure 3). Therefore, the position of this equilibrium, and the chemical shifts seen in the NMR spectra of these complexes, may be influenced not only by typical factors such as temperature or concentration but also by the chirality of the complexes undergoing dimerization due to the relative stability of the hetero and homochiral dimers as discussed above. This could help explain the disparities seen in the NMR spectra of the racemic and enantiopure complexes.

Pulsed Field Gradient Spin Echo (PGSE) NMR spectroscopy is often used to probe the nuclearity of compounds in solution via the determination of their diffusion coefficients (*D_i*) and therefore their hydrodynamic radii (*r_H*) and comparing these to other calculated radii, such as those

estimated from x-ray crystallographic data (r_{xray}).⁵⁶⁻⁶⁰ Differences of ~15 – 20% in the diffusion coefficients of two species can be considered to be representative of a change in the molecular volume by a factor of 2 (e.g. a change from monomer to dimer).^{57,58} In fluxional systems, such as those with a monomer-dimer equilibrium, the calculated diffusion coefficients and hydrodynamic radii represent average values dependent upon the composition of monomers/dimers in solution under the experimental conditions used.^{59,60}

Recently, we used PGSE NMR experiments to confirm the nuclearity of our parent *t*-butyl substituted complexes (\pm)-(NNO_{*t*Bu})InCl₂ and (\pm)-[(NNO_{*t*Bu})InCl]₂(μ -Cl)(μ -OEt) in solution (Table 1, entries 1, 4-5).⁴⁸ In this case, the diffusion coefficient of the dichloride complex is 14% smaller than the corresponding proligand, but that of the ethoxide-bridged complex is 25% smaller than the dichloride complex. This suggests the dichloride is mononuclear in solution (or if the system is fluxional as reported here, that the major species in solution is the monomeric complex) while the ethoxide complex remains dinuclear. These results are further supported by the good agreement between the calculated hydrodynamic radii of the complexes and the radii estimated from the solid-state structure of (\pm)-(NNO_{*t*Bu})InMe₂ (used as an approximation of (\pm)-(NNO_{*t*Bu})InCl₂ as the structure of this complex is not available) and the dinuclear solid-state structure of (\pm)-[(NNO_{*t*Bu})InCl]₂(μ -Cl)(μ -OEt) (Table 1, entries 4-5).

In order to probe the nuclearity of the new indium dichloride complexes in solution, the diffusion coefficients (D_i) and hydrodynamic radii (r_{H}) of the racemic and enantiopure silyl substituted dichloride complexes, (\pm)- and (*R,R*)-**1**, and the adamantyl substituted complex (\pm)-**2** were determined using PGSE NMR spectroscopy. PGSE NMR data was also collected for the corresponding proligands (\pm)-H(NNO_{SiPh₃}) and (\pm)-H(NNO_{Ad}), as a low estimate of values corresponding to the monomeric species, and the ethoxide complex (\pm)-[(NNO_{SiPh₃})InCl]₂(μ -Cl)(μ -OEt) (**4**) (see below), as an estimate of values corresponding to the dimeric species. The aforementioned data for the parent *t*-butyl substituted ligand and indium complexes was also used for comparison (Table 1).

Table 1. Diffusion coefficients and radii for select species determined by PGSE NMR spectroscopy.^a

Compound	D_i (10 ⁻¹⁰ m ² s ⁻¹) ^b	r_{H} (Å) ^c	r_{xray} (Å) ^d
1 (\pm)-H(NNO _{<i>t</i>Bu}) ⁴⁸	12.0	5.2	–
2 (\pm)-H(NNO _{Ad})	10.2	6.0	–
3 (\pm)-H(NNO _{SiPh₃})	9.1	6.3	–
4 (\pm)-(NNO _{<i>t</i>Bu})InCl ₂ ⁴⁸	10.4	5.9	5.4 ^e
5 (\pm)-[(NNO _{<i>t</i>Bu})InCl] ₂ (μ -Cl)(μ -OEt) ⁴⁸	7.8	7.5	7.3
6 (\pm)-(NNO _{Ad})InCl ₂ (2)	9.1	6.4	8.0
7 (\pm)-(NNO _{SiPh₃})InCl ₂ (1)	7.1	8.0	7.3
8 (<i>R,R</i>)-(NNO _{SiPh₃})InCl ₂ (1)	7.0	8.0	–
9 (\pm)-[(NNO _{SiPh₃})InCl] ₂ (μ -Cl)(μ -OEt) (4)	6.5	8.6	–

^a[Compound] = 4.5 mM in 1 mL of a 0.94 mM CD₂Cl₂ solution of tetrakis(trimethylsilyl)silane (TMSS) as an internal standard; ^bCalculated from the slopes of the linear portions of the plots of $\ln(I/I_0)$ vs. $\gamma^2 \delta^2 G^2 [\Delta(\delta/3)] \times 10^{10}$ (m⁻² s) from PGSE NMR experiments (see SI, Figure S10); ^cCalculated from the observed D_i values and the modified Stokes-Einstein equation according to the literature (see SI for detailed procedure);^{56,57,60} ^dCalculated, where applicable, from the volume (V) of the crystal structure unit cell as well as the number of molecules of the compound of interest (n) occupying the unit cell assuming a spherical shape $r_{\text{xray}} = (3V/4\pi n)^{1/3}$ (see SI for detailed procedure); ^eValue is for complex (\pm)-(NNO_{*t*Bu})InMe₂ as solid-state structural data for (\pm)-(NNO_{*t*Bu})InCl₂ is not available.

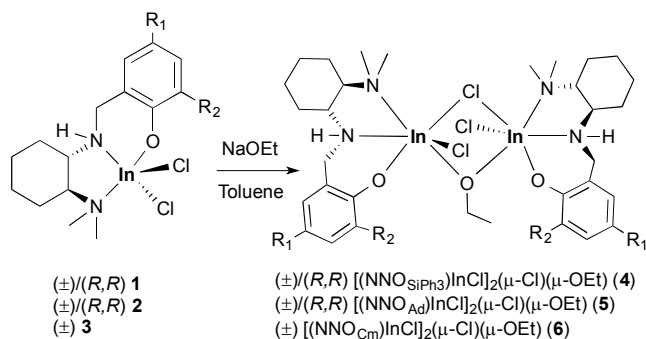
The observed diffusion coefficients for the *t*-butyl,⁴⁸ adamantyl, and silyl substituted proligands are 12.0, 10.2, and 9.1 ($\times 10^{-10}$ m²s⁻¹) respectively and are inversely correlated to the increasing steric bulk of the compounds (Table 1, entries 1-3). The hydrodynamic radii are calculated from the D_i values and are necessarily larger for the larger species.

A comparison of the diffusion coefficients for the silyl substituted dichloride complexes (\pm)- and (*R,R*)-**1** shows a difference of >20% between these species and the corresponding proligand, suggesting that the major species in solution is dinuclear, presumably the heterochiral dimer for the racemic complex and the homochiral dimer for the enantiopure complex (Table 1, entries 3 and 7-8). This is not surprising, as the corresponding chemical shift differences and multiplicities of the methylene protons in both silyl substituted analogues (Figure 3) are similar to the related indium ethoxide complex (\pm)-**4** (see below), which has a similar diffusion coefficient to complexes (\pm)- and (*R,R*)-**1** and is therefore also proposed to be dinuclear in solution (Table 1, entries 7-9). In contrast, the diffusion coefficient of the adamantyl substituted dichloride complex (\pm)-**2** is similar to the parent system and shows a difference of only 11% from the corresponding proligand, suggesting the major species in solution is mononuclear (Table 1, entries 2 and 6). These observations are further supported by the good agreement between the calculated hydrodynamic radii (r_{H}) of complexes (\pm)- and (*R,R*)-**1** with the radius estimated from the dinuclear solid-state structure (r_{xray}) of (*RR/SS*)-**1** (Table 1, entries 7-8). Conversely, there is poorer agreement between the r_{H} of (\pm)-**2** and the r_{xray} of dinuclear (*RR/SS*)-**2** (Table 1, entry 6), consistent with the dominant species in solution being monomeric.

The disparity in chemical shifts between (\pm)-**2** and (*R,R*)-**2** may be caused by a combination of slightly different ratios of

monomers/dimers in solution for both species (assuming fast exchange⁵⁹), even if the dominant species is monomeric in both cases, and the difference in the structures of the presumed dimeric species that would form from the racemic and enantiopure analogues (hetero vs. homochiral respectively). Considering the differences between the chemical shifts of the methylene protons of the silyl substituted analogues, where the dominant species is dinuclear, and the relative similarities in chemical shift differences and multiplicities of the methylene protons of the adamantyl and *t*-butyl analogues, where the dominant species is mononuclear, and the cumyl dichloride complexes we can hypothesize that the cumyl analogues may also be predominantly mononuclear in solution, albeit to different degrees for the racemic versus enantiopure analogues as discussed above (Figure 3).

Salt metathesis of complexes (\pm)- or (*R,R*)- **1-3** with NaOEt yields the dinuclear indium ethoxide complexes (\pm)- or (*R,R*)- [(NNO_R)InCl]₂(μ -Cl)(μ -OEt) (R = SiPh₃, **4**; Ad, **5**; Cm, **6**) in isolated yields of 42–58 % (Scheme 3). Due to the insufficient purity of enantiopure complex (*R,R*)-**3**, complex (*R,R*)-**6** was not synthesized and will not be discussed further. The ¹H NMR spectra of the resulting enantiopure and racemic complexes are identical and show the μ -OCH₂CH₃ protons as two sets of multiplets at ~ 4 ppm (see SI, Figures S7–9). These are flanked by the diastereotopic N-CH₂-Ar protons of the ligand backbone which appear as doublets at ~ 5 and 3.5 ppm. A similar pattern of resonances are observed for other dimeric mono-alkoxy bridged complexes [(NNO_{tBu})InX]₂(μ -X)(μ -OEt) (X = Cl, Br, I).^{44–46,48,50} As described above, the dinuclear nature of complex (\pm)-**4** in solution can be confirmed by PGSE NMR spectroscopy.



Scheme 3. Synthesis of indium ethoxide complexes with various phenolate substituents.

Single crystals of complexes (\pm)-**5** and (\pm)-**6** can be obtained at room temperature from saturated solutions of the complexes in acetonitrile and toluene, respectively. Their molecular structures, determined using single crystal X-ray crystallography, are in agreement with previous compounds in the series and show that complexes (\pm)-**5** and (\pm)-**6** crystallize as homochiral dimers (Figure 4). Both indium centers have distorted octahedral geometry and display similar bond lengths and angles around the central core of the molecules (Figure 4; Table S1).

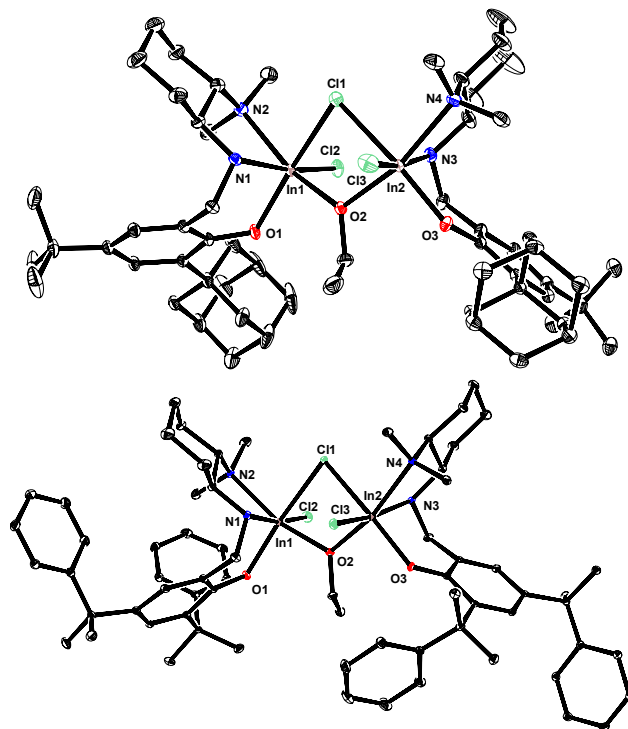


Figure 4. Solid-state molecular structures of complexes (\pm)-**5** (top) and (\pm)-**6** (bottom). The structures are depicted with thermal ellipsoids at 50% probability and solvent and H atoms omitted for clarity. Selected bond lengths (Å) for complex (\pm)-**5**: In1–N1 2.2708(16), In1–N2 2.3806(17), In1–O1 2.0792(13), In1–O2 2.1411(13), In1–Cl1 2.6525(5), In1–Cl2 2.4221(5), In2–N3 2.2594(16), In2–N4 2.3680(16), In2–O3 2.0590(13), In2–O2 2.1486(13), In2–Cl1 2.6523(5), In2–Cl3 2.4200(5); for complex (\pm)-**6**: In1–N1 2.2769(17), In1–N2 2.3468(18), In1–O1 2.0902(14), In1–O2 2.1308(15), In1–Cl1 2.7023(9), In1–Cl2 2.4218(9), In2–N3 2.2721(17), In2–N4 2.3554(17), In2–O3 2.0748(15), In2–O2 2.1288(15), In2–Cl1 2.6388(8), In2–Cl3 2.4301(8). Selected bond angles (°) for complex (\pm)-**5**: In1–Cl1–In2 86.835(15), In1–O2–In2 116.42(6), O1–In1–N1 87.86(5), O2–In1–N1 94.42(5), O1–In1–N2 104.55(5), O2–In1–N2 160.08(4), N1–In1–N2 76.07(6), N1–In1–Cl2 168.08(4), N2–In1–Cl2 92.03(4), O1–In1–Cl1 165.13(4), O2–In1–Cl1 77.31(4), O3–In2–N3 87.88(6), O2–In2–N3 91.83(5), O3–In2–N4 99.38(6), O2–In2–N4 160.64(5), N3–In2–N4 76.60(6), N3–In2–Cl3 169.65(4), N4–In2–Cl3 93.42(4), O3–In2–Cl1 168.94(4), O2–In2–Cl1 77.19(4); for complex (\pm)-**6**: In1–Cl1–In2 86.076(19), In1–O2–In2 117.71(6), O1–In1–N1 87.26(6), O2–In1–N1 92.41(6), O1–In1–N2 102.35(6), O2–In1–N2 159.88(6), N1–In1–N2 76.57(6), N1–In1–Cl2 169.87(4), N2–In1–Cl2 94.42(4), O1–In1–Cl1 165.17(4), O2–In1–Cl1 76.73(4), O3–In2–N3 87.36(6), O2–In2–N3 95.13(6), O3–In2–N4 100.99(6), O2–In2–N4 163.22(6), N3–In2–N4 76.48(6), N3–In2–Cl3 169.13(4), N4–In2–Cl3 92.66(4), O3–In2–Cl1 166.05(4), O2–In2–Cl1 78.21(4).

Polymerization studies.

Bulk polymerizations of *rac*-LA with the racemic complexes (\pm)-**4-6** with various equivalents of monomer show molecular weights (M_n) fairly consistent with theoretical values and low polydispersities (PDI) (Table 2). The adamantyl and cumyl catalysts (\pm)-**5** and **6** show slight isotactic biases, with P_m values of ~ 0.6 (Table 2, entries 3–6), which are comparable to (\pm)-[(NNO_{tBu})InCl]₂(μ -Cl)(μ -OEt) under similar conditions.^{44,48} In contrast, catalyst (\pm)-**4** shows reduced isoselectivity, with P_m values indicative of essentially atactic polymers (0.53). The enantiopure complex (*R,R*)-**4** shows a slight heterotactic bias (P_m ~ 0.44). A similar situation is observed with the parent

catalyst, where enantiopure $[(\text{NNO}_{i\text{Bu}})\text{InCl}]_2(\mu\text{-Cl})(\mu\text{-OEt})$ displays reduced isoselectivity ($P_m \sim 0.5$) compared to the racemic catalyst ($P_m \sim 0.6$).^{44,48}

Table 2. Results for the polymerization of *rac*-LA by catalysts (\pm)-**4-6**.^a

Entry	Catalyst	$[\text{LA}]_0/[\text{cat.}]$	$M_n^{\text{theo}^b}$ (gmol^{-1})	$M_n^{\text{GPC}^c}$ (gmol^{-1})	PDI ^c	P_m^d
1	(\pm)- 4	550	76000	84270	1.04	0.53
2	(\pm)- 4	930	130000	153100	1.02	0.53
3	(\pm)- 5	530	73000	53100	1.04	0.58
4	(\pm)- 5	820	110000	96680	1.08	0.58
5	(\pm)- 6	540	77000	68930	1.03	0.58
6	(\pm)- 6	880	120000	86220	1.16	0.57

^aPolymerizations reached >94% conversion (determined by ¹H NMR spectroscopy); ^bCalculated from $[\text{LA}]_0/[\text{initiator}] \times \text{LA conversion} \times M_{\text{LA}} (144.13) + M_{\text{Endgroups}} (46.07)$; ^cDetermined by GPC measurements in THF; ^dDetermined by ¹H{¹H} NMR spectroscopy and Bernoullian statistics.

The polymerization of *rac*-, L- and D-LA with catalysts (\pm)- and (*R,R*)- **4** and **5** and (\pm)-**6** can be studied at room temperature in CDCl₃ via *in situ* ¹H NMR spectroscopy. The plots of $\ln([\text{LA}])$ versus time show slow initiation periods followed by first order propagation from which k_{obs} data can be extracted (Table 3, Figures S11-15). These reactions are monitored in an NMR tube, and the conversion is determined based on the integration of monomer peaks compared to an internal standard. Based on these spectra, there may be some unreacted catalyst in each of the samples generated by **4**, **5** and **6**, as well as $[(\text{NNO}_{i\text{Bu}})\text{InCl}]_2(\mu\text{-Cl})(\mu\text{-OEt})$, however it is impossible to quantify the amount of unreacted catalyst in these systems under these conditions due to overlap of their peaks with those of the polymeryl species (Figures S16-20). This may account for the slight differences in rate between the different catalysts shown in Table 3.

The dilute catalyst concentrations (~2 mM) used in these experiments, as well as the absence of precipitate formation during polymerization, indicate that poor solubility of the catalysts is unlikely to be the cause of these observations. Indeed, monitoring the polymerization of *rac*-LA with catalyst (\pm)-**4** in CD₂Cl₂, in which the catalyst has higher solubility versus CDCl₃, does not appear to affect the observed rate constants (Table 3 and Figures S11-12).

The racemic catalysts show no preference for the polymerization of either the L- or D-lactide, resulting in k_L/k_D (k_{rel}) values of ~1 for all four systems (Table 3, entries 2-3, 8-9, 14-15, 20-21). The polymerization of *rac*-LA with (\pm)-**4-6** is slightly slower than with L- or D-LA, in line with observations of the parent complex $[(\text{NNO}_{i\text{Bu}})\text{InCl}]_2(\mu\text{-Cl})(\mu\text{-OEt})$ (Table 3, entries 1, 7, 13 and 19).⁴⁸ Only the silyl substituted catalyst (\pm)-**4** deviates from this trend, with observed rate constants equal, within error, for *rac*-, L- and D-LA. As mentioned above, the racemic complexes are all homochiral dimers, thus the slower rates of *rac*-LA polymerization over L- or D-LA polymerization with (\pm)-**5-6** may be due to catalyst inhibition by the mismatched monomer, as was proposed for the parent

catalyst.⁴⁸ This may not be the case for catalyst (\pm)-**4** due to a lower selectivity between L- and D-LA, as noted below.

As with the parent complex $[(\text{NNO}_{i\text{Bu}})\text{InCl}]_2(\mu\text{-Cl})(\mu\text{-OEt})$, the enantiopure catalysts (*R,R*)-**4** and **5** show higher rates of polymerization for L-LA compared to D-LA with k_{rel} values of 12 and 6 respectively (Table 3, entries 11-12 and 17-18). The kinetic behavior of the adamantyl catalyst (*R,R*)-**5** is similar to the parent system which has a k_{rel} of 14 (Table 3, entries 5-6).⁴⁸ The magnitude and trends in the kinetic data as well as the catalyst molecular weight control and stereoselectivity are also very similar between the two catalyst systems.

These data show that making large changes to the *ortho* phenolate substituent in these complexes has an impact on polymer tacticity. Polymerization of *rac*-LA with the silyl substituted catalyst (\pm)-**4** yields essentially atactic PLA ($P_m \sim 0.5$). Although there is still a preference for L-LA with (*R,R*)-**4**, the k_{rel} of 6 is significantly lower than that for (*R,R*)-**5** or the parent complex and clearly demonstrates the importance of the *ortho* phenolate substituent in determining the stereoselectivity of these systems.

A possible explanation for this reduction in selectivity for a catalyst with a bulkier group may be catalyst dissociation in solution in the presence of lactide. Previous studies in our group attributed a loss of stereoselectivity in the polymerization of *rac*-LA upon increasing the steric bulk of the terminal amine substituents of the parent catalyst system (from methyl to *n*-propyl) to a change in the nuclearity of the complex during polymerization.⁴⁶ The clear observation of the dichloride species during *in situ* monitoring of the polymerization confirmed that the bulkier *n*-propyl groups caused dissociation of the dimeric catalyst during polymerization and a corresponding loss of stereoselectivity.⁴⁶ Although the PGSE NMR spectroscopic data for catalyst (\pm)-**4** suggest a dinuclear structure in solution, this is in the absence of added monomer. The ¹H NMR spectra of the polymerization of *rac*-LA by catalyst (\pm)-**4** (in either CDCl₃ or CD₂Cl₂) shows the presence of the dichloride complex (\pm)-**1**, although extensive overlap of the peaks for (\pm)-**1** with the polymeryl species make quantitative estimates of dissociation difficult (Figures S16-17). This suggests that disruption of the nuclearity of complex (\pm)-**4** during polymerization may also be the reason for its reduced stereoselectivity in the polymerization of *rac*-LA.

Table 3. Effects of catalyst structure and chirality on the kinetics of the polymerization of *rac*, L and D-LA by (\pm)/(*R,R*) [(NNO_{SiPh₃})InCl]₂(μ -Cl)(μ -OEt) (parent),⁴⁸ **4** and **5** and (\pm)-**6**.^a

	Catalyst	Monomer	$k_{\text{obs}} (\times 10^{-3} \text{ s}^{-1})^b$	$k_{\text{rel}} (k_{\text{I}}/k_{\text{D}})$
1	(\pm)-parent	<i>rac</i> -LA	1.7	1
2	(\pm)-parent	L-LA	3.0	
3	(\pm)-parent	D-LA	3.0	
4	(<i>R,R</i>)-parent	<i>rac</i> -LA	0.62 (0.21) ^c	14
5	(<i>R,R</i>)-parent	L-LA	3.4	
6	(<i>R,R</i>)-parent	D-LA	0.25	
7	(\pm)- 4	<i>rac</i> -LA	1.0 (0.91) ^d	1
8	(\pm)- 4	L-LA	1.1	
9	(\pm)- 4	D-LA	1.2	
10	(<i>R,R</i>)- 4	<i>rac</i> -LA	0.40 (0.52) ^d	6
11	(<i>R,R</i>)- 4	L-LA	1.5 (1.7) ^d	
12	(<i>R,R</i>)- 4	D-LA	0.24	
13	(\pm)- 5	<i>rac</i> -LA	2.4	1
14	(\pm)- 5	L-LA	3.4	
15	(\pm)- 5	D-LA	3.4	
16	(<i>R,R</i>)- 5	<i>rac</i> -LA	0.74	12
17	(<i>R,R</i>)- 5	L-LA	3.4	
18	(<i>R,R</i>)- 5	D-LA	0.28	
19	(\pm)- 6	<i>rac</i> -LA	1.4	1
20	(\pm)- 6	L-LA	1.7	
21	(\pm)- 6	D-LA	1.8	

^aAll polymerization were carried out with 200 eq. LA and followed by *in situ* ¹H NMR spectroscopy (400 MHz, CDCl₃, 25 °C) to over 90% conversion with [LA] = 0.48 M and [cat] = 2.4 mM and 1,3,5-trimethoxybenzene (0.03 M) used as an internal standard; ^bDetermined from the negative of the slope of the linear portions of the plots of ln([LA]) vs. time; ^cThere are two linear regions in the plot of ln([LA]) vs. time for this catalyst, with a faster rate (0.62) up to ~30 min. then a sharp decrease to a lower rate (0.21) after 30 min.;⁴⁸ ^dValues in parentheses were measured in CD₂Cl₂ under similar conditions.

Conclusions

In this study we set out to investigate the role of the phenolate substituents and the chirality of our tridentate ligand system on the stereoselectivity of dinuclear indium alkoxide catalysts for the ring opening polymerization of *rac*-LA. To this end, we synthesized a family of racemic and enantiopure diamino-phenolate proligands with various phenolate substituents and used them to generate a family of indium dichloride complexes as intermediates towards the synthesis of active indium alkoxide complexes.

We observed a difference in the nuclearity of the indium dichloride complexes with changes to the *ortho*-phenolate substituent. In contrast to previously reported dihalide complexes made with the parent *ortho/para* di-*t*-butyl substituted ligand system, the dichloride complexes discussed in this paper, namely complexes (\pm)-(NNO_{SiPh₃})InCl₂ (**1**) and (\pm)-(NNO_{Ad})InCl₂ (**2**), were dinuclear in the solid-state, forming heterochiral (*RR/SS*) dimers bridged by chloride ligands. Solution state ¹H and PGSE NMR spectroscopy confirmed that these complexes are most likely undergoing fast exchange between the monomeric and dimeric forms in solution, with the position of the equilibrium depending not only on concentration and temperature but also the chirality of

the complexes undergoing aggregation. The results indicate that (\pm)- and (*R,R*)-**1** most likely exist as predominantly the dinuclear structure in solution, whereas complexes (\pm)- and (*R,R*)-**2** and **3** were more likely to be monomeric in solution. Interestingly, this penchant for aggregation was independent of the steric bulk of the *ortho*-phenolate group.

The polymerization of *rac*-LA with (\pm)-**4-6** indicated that all three catalysts are relatively well controlled, producing polymers with controlled molecular weights and low PDI values. The adamantyl and cumyl substituted analogues **5** and **6** had similar stereoselectivity to the parent system, yielding isotactically enriched PLA ($P_m \sim 0.6$). In contrast, the silyl substituted analogue (**4**), was less stereoselective, with the racemic catalyst producing essentially atactic PLA ($P_m \sim 0.5$).

The difference in behaviour of the silyl substituted catalyst extends to the rates of polymerization. A comparison of the rates of polymerization of L- and D-LA with (*R,R*)-**4** and **5** showed that while the adamantyl substituted complex **5** had a k_{rel} of ~12, which is similar to the value observed for the parent system (14), the silyl substituted catalyst **4** had a significantly reduced k_{rel} value of ~6. In previously reported systems with significantly bulky groups we have attributed the loss in selectivity to catalyst dissociation. We did find convincing evidence of catalyst dissociation during polymerization for catalyst **4**, although the extent of this dissociation is difficult to quantify due to significant overlap of the peaks for the dissociation product (complex **1**) with the polymeryl species (Figures S16-17).

We can conclude that changing the steric bulk and/or electronic properties of the phenolate substituents in this tridentate ligand system does not lead to more active and/or stereoselective indium catalysts for lactide polymerization. Our experience with the different indium complexes made within this tridentate ligand family show that the different aggregation modes and the degrees of freedom possible for these indium complexes will complicate any effort to enhance selectivity using this ligand system. Therefore, other avenues towards producing more selective catalysts are being pursued.

Experimental

General methods.

Unless otherwise specified all air and/or water sensitive reactions were carried out using standard Schlenk techniques under N₂ or in a N₂ filled MBraun glovebox. A Bruker Avance 600 MHz spectrometer was used to record the ¹H NMR, ¹³C{¹H} NMR, and ¹H{¹H} NMR spectra. ¹H NMR chemical shifts are given in ppm versus residual protons in deuterated solvents as follows: δ 5.32 for CD₂Cl₂ and δ 7.27 for CDCl₃. ¹³C{¹H} NMR chemical shifts are given in ppm versus residual ¹³C in solvents as follows: δ 54.00 for CD₂Cl₂ and δ 77.23 for CDCl₃. Diffraction measurements for X-ray crystallography were made on a Bruker X8 APEX II diffraction with graphite monochromated Mo-K α radiation. The structures were solved by direct methods and refined by full-matrix least-squares using

the SHELXTL crystallographic software of the Bruker-AXS. Unless specified, all non-hydrogens were refined with anisotropic displacement parameters, and all hydrogen atoms were constrained to geometrically calculated positions but were not refined. EA CHN analysis was performed using a Carlo Erba EA1108 elemental analyzer. The elemental composition of an unknown sample was determined by using a calibration factor. The calibration factor was determined by analyzing a suitable certified organic standard (OAS) of a known elemental composition. Molecular weights were determined using an Agilent 1200 Series pump and autosampler, Phenomenex columns (Phenogel 5 μ m 10E4A LC Column 300 \times 4.6 mm, 5 K - 500 K MW; Phenogel 5 μ m 10E3A LC Column 300 \times 4.6 mm, 1K - 75K MW; Phenogel 5 μ m 500 \AA LC Column 300 \times 4.6 mm, 1K - 15K MW), Wyatt Optilab rEX (refractive index detector $\lambda = 690$ nm, 40 $^{\circ}$ C), Wyatt tristar miniDAWN (laser light scattering detector operating at $\lambda = 690$ nm), and a Wyatt ViscoStar viscometer. The column temperature was set at 40 $^{\circ}$ C. A flow rate of 0.5 mL/min was used and samples were dissolved in THF (ca. 2 mg/mL) and a dn/dc value of 0.042 mL/g was used. Narrow molecular weight polystyrene standards were used for calibration purposes.

Materials

Toluene, diethyl ether, hexane, and tetrahydrofuran were degassed and dried using alumina columns in a solvent purification system. The tetrahydrofuran was further dried over sodium/benzophenone and vacuum transferred to a Straus flask and degassed prior to use. In addition CH_3CN and CH_2Cl_2 were refluxed over CaH_2 in a solvent still and transferred to a Straus flask where they were degassed prior to use. Deuterated solvents were dried over CaH_2 and vacuum-transferred to a Straus flask and then degassed through a series of freeze-pump-thaw cycles. Deuterium-labelled NMR solvents were purchased from Cambridge Isotope Laboratory or Aldrich. InCl_3 was obtained from Strem Chemicals and used without further purification. Potassium *t*-butoxide was sublimed prior to use. (\pm)- and (*R,R*)-*N,N*-dimethyl-*trans*-1,2-diaminocyclohexane, 2-hydroxy-5-methyl-3-(triphenylsilyl)benzaldehyde, 2-hydroxy-3,5-bis(2-phenylpropan-2-yl)benzaldehyde and 3-((3*r*,5*r*,7*r*)-adamantan-1-yl)-5-(*t*-butyl)-2-hydroxybenzaldehyde were prepared according to modified literature procedures.^{52-54,61} Lactide samples were obtained from Purac Biomaterials and recrystallized several times from hot toluene and dried under vacuum prior to use.

General procedure for synthesis of imines. The desired amine (\pm)- or (*R,R*)-*N,N*-dimethyl-*trans*-1,2-diaminocyclohexane (9.60 mmol) was transferred using methanol (25 mL) to a solution of the appropriate salicylaldehyde (8.00 mmol) in methanol (25 mL). The mixture was stirred for 18 h at room temperature. The resulting suspension was either filtered yielding the crude product as a yellow solid or pumped to dryness yielding the crude product as a yellow foamy residue depending on the solubility of the

imine. Further purification was achieved through recrystallization in a variety of solvents (see below for details).

Synthesis of 2-(((\pm)-*trans*-2-(dimethylamino)cyclohexylimino)methyl)-4-methyl-6-(triphenylsilyl)phenol.

The title compound was isolated as a bright yellow solid after filtration of the crude reaction mixture. The crude solid was dissolved in a minimum of hot methanol and the solution was cooled to 0 $^{\circ}$ C causing precipitation of the pure product, which was isolated via vacuum filtration as a yellow solid and dried under vacuum prior to use (1.42 g, 86 %). ^1H NMR (600 MHz, 25 $^{\circ}$ C, CDCl_3): δ 8.30 (1H, s, $\text{CH}=\text{N}$), 7.64 (6H, m, SiPh_3), 7.36 (9H, m, SiPh_3), 7.15 (1H, m, *Ar-H*), 7.01 (1H, m, *Ar-H*), 3.22 (1H, m, *CHN*), 2.54 (1H, m, *CHN*), 2.25 (6H, s, $\text{N}(\text{CH}_3)_2$), 2.19 (3H, s, *Ar-CH}_3*), 1.79 (3H, m, DACH), 1.71 (1H, m, DACH), 1.54 (1H, m, DACH), 1.26 (3H, m, DACH). $^{13}\text{C}\{^1\text{H}\}$ NMR (150 MHz, 25 $^{\circ}$ C, CDCl_3): δ 164.5, 163.1, 141.6, 136.4, 134.9, 133.9, 129.2, 127.6, 126.9, 121.2, 118.0, 70.0, 66.6, 40.8, 34.7, 25.3, 25.2, 24.5, 20.5. Anal. Calc. for $\text{C}_{34}\text{H}_{38}\text{N}_2\text{OSi}$: C, 78.72; H, 7.38; N, 5.40. Found: C, 78.80; H, 7.32; N, 5.17.

Synthesis of 2-(((*R,R*)-*trans*-2-(dimethylamino)cyclohexylimino)methyl)-4-methyl-6-(triphenylsilyl)phenol.

The title compound was isolated as a bright yellow solid after filtration of the crude reaction mixture. The solid was dried under vacuum with no further purification necessary (1.016 g, 78 %). ^1H NMR (600 MHz, 25 $^{\circ}$ C, CDCl_3): δ 8.29 (1H, s, $\text{CH}=\text{N}$), 7.64 (6H, m, SiPh_3), 7.35 (9H, m, SiPh_3), 7.16 (1H, m, *Ar-H*), 7.01 (1H, m, *Ar-H*), 3.22 (1H, m, *CHN*), 2.53 (1H, m, *CHN*), 2.25 (6H, s, $\text{N}(\text{CH}_3)_2$), 2.19 (3H, s, *Ar-CH}_3*), 1.78 (3H, m, DACH), 1.71 (1H, m, DACH), 1.54 (1H, m, DACH), 1.27 (3H, m, DACH). $^{13}\text{C}\{^1\text{H}\}$ NMR (150 MHz, 25 $^{\circ}$ C, CDCl_3): δ 164.5, 163.1, 141.6, 136.4, 134.9, 133.9, 129.2, 127.6, 126.9, 121.2, 118.0, 70.0, 66.6, 40.8, 34.7, 25.3, 25.2, 24.5, 20.4. Anal. Calc. for $\text{C}_{34}\text{H}_{38}\text{N}_2\text{OSi}$: C, 78.72; H, 7.38; N, 5.40. Found: C, 78.85; H, 7.27; N, 5.08.

Synthesis of 2-(((\pm)-*trans*-2-(dimethylamino)cyclohexylimino)methyl)-4-*t*-butyl-6-(adamantan-1-yl)phenol.

The reaction mixture was filtered yielding the title compound as a yellow solid. This solid was dried under vacuum with no further purification necessary (2.06 g, 74 %). ^1H NMR (600 MHz, 25 $^{\circ}$ C, CDCl_3): δ 8.31 (1H, s, $\text{CH}=\text{N}$), 7.30 (1H, m, *Ar-H*), 7.07 (1H, m, *Ar-H*), 3.20 (1H, m, *CHN*), 2.64 (1H, m, *CHN*), 2.29 (6H, s, $\text{N}(\text{CH}_3)_2$), 2.20 (6H, m, Ad), 2.10 (3H, m, Ad), 1.88 (1H, m, DACH), 1.81 (9H, m, Ad + DACH), 1.66 (1H, m, DACH), 1.32 (9H, s, $\text{C}(\text{CH}_3)_3$), 1.30 (3H, m, DACH). $^{13}\text{C}\{^1\text{H}\}$ NMR (150 MHz, 25 $^{\circ}$ C, CDCl_3): δ 164.3, 158.6, 139.7, 136.8, 126.5, 125.6, 118.1, 69.8, 66.7, 40.8, 40.3, 37.2, 35.0, 34.1, 31.5, 29.1, 25.2, 24.7, 23.9. Anal. Calc. for $\text{C}_{29}\text{H}_{44}\text{N}_2\text{O}$: C, 79.76; H, 10.16; N, 6.42. Found: C, 79.92; H, 10.37; N, 6.28.

Synthesis of 2-(((*R,R*)-*trans*-2-(dimethylamino)cyclohexylimino)methyl)-4-*t*-butyl-6-(adamantan-1-yl)phenol.

The reaction mixture was filtered yielding the title

compound as a yellow solid. This solid was dried under vacuum with no further purification necessary (0.552 g, 77 %). ^1H NMR (600 MHz, 25 °C, CDCl_3): δ 8.31 (1H, s, $\text{CH}=\text{N}$), 7.31 (1H, m, Ar-*H*), 7.07 (1H, m, Ar-*H*), 3.20 (1H, m, *CHN*), 2.64 (1H, m, *CHN*), 2.28 (6H, s, $\text{N}(\text{CH}_3)_2$), 2.20 (6H, m, Ad), 2.10 (3H, m, Ad), 1.88 (1H, m, DACH), 1.81 (9H, m, Ad + DACH), 1.65 (1H, m, DACH), 1.32 (9H, s, $\text{C}(\text{CH}_3)_3$), 1.30 (3H, m, DACH). $^{13}\text{C}\{^1\text{H}\}$ NMR (150 MHz, 25 °C, CDCl_3): δ 164.3, 158.6, 139.7, 136.8, 126.5, 125.6, 118.0, 69.8, 66.7, 40.8, 40.3, 37.2, 35.0, 34.2, 31.5, 29.1, 25.2, 24.7, 23.9. Anal. Calc. for $\text{C}_{29}\text{H}_{44}\text{N}_2\text{O}$: C, 79.76; H, 10.16; N, 6.42. Found: C, 79.60; H, 10.35; N, 6.01.

Synthesis of 2-(((±)-*trans*-2-(dimethylamino)cyclohexylimino)methyl)-4,6-bis(2-phenylpropan-2-yl)phenol. The title compound was isolated as a yellow solid after filtration of the crude reaction mixture. The solid was dried under vacuum with no further purification necessary (2.199 g, 80 %) ^1H NMR (600 MHz, 25 °C, CDCl_3): δ 8.20 (1H, s, $\text{CH}=\text{N}$), 7.29 (5H, m, Ar-*H* + $\text{C}(\text{CH}_3)_2\text{Ph}$), 7.21 (5H, m, $\text{C}(\text{CH}_3)_2\text{Ph}$), 7.13 (1H, m, $\text{C}(\text{CH}_3)_2\text{Ph}$), 7.01 (1H, m, Ar-*H*), 3.11 (1H, m, *CHN*), 2.52 (1H, m, *CHN*), 2.20 (6H, s, $\text{N}(\text{CH}_3)_2$), 1.78 (5H, m, *NH* + DACH), 1.71 (6H, s, $\text{C}(\text{CH}_3)_2\text{Ph}$), 1.69 (3H, s, $\text{C}(\text{CH}_3)_2\text{Ph}$), 1.66 (3H, s, $\text{C}(\text{CH}_3)_2\text{Ph}$), 1.50 (1H, m, DACH), 1.21 (3H, m, DACH). $^{13}\text{C}\{^1\text{H}\}$ NMR (150 MHz, 25 °C, CDCl_3): δ 163.7, 158.0, 150.9, 150.7, 139.1, 135.9, 128.7, 128.0, 127.8, 127.6, 126.8, 125.6, 125.6, 125.0, 118.2, 69.8, 66.5, 42.4, 42.2, 40.6, 34.9, 31.0, 30.9, 29.7, 29.2, 25.2, 24.6, 23.8. Anal. Calc. for $\text{C}_{33}\text{H}_{42}\text{N}_2\text{O}$: C, 82.11; H, 8.77; N, 5.80. Found: C, 82.11; H, 8.41; N, 5.69.

Synthesis of 2-(((*R,R*)-*trans*-2-(dimethylamino)cyclohexylimino)methyl)-4,6-bis(2-phenylpropan-2-yl)phenol. The reaction mixture was pumped to dryness *in vacuo* yielding the crude product as a yellow foamy residue. This residue was dissolved in a minimum of hot petroleum ether and the solution was cooled to 0 °C causing the precipitation of the pure product, which was isolated via vacuum filtration as a yellow solid and dried under vacuum prior to use (0.555 g, 41 %) ^1H NMR (600 MHz, 25 °C, CDCl_3): δ 8.18 (1H, s, $\text{CH}=\text{N}$), 7.28 (5H, m, Ar-*H* + $\text{C}(\text{CH}_3)_2\text{Ph}$), 7.19 (5H, m, $\text{C}(\text{CH}_3)_2\text{Ph}$), 7.11 (1H, m, $\text{C}(\text{CH}_3)_2\text{Ph}$), 6.99 (1H, m, Ar-*H*), 3.09 (1H, m, *CHN*), 2.50 (1H, m, *CHN*), 2.17 (6H, s, $\text{N}(\text{CH}_3)_2$), 1.77 (5H, m, *NH* + DACH), 1.69 (6H, s, $\text{C}(\text{CH}_3)_2\text{Ph}$), 1.67 (3H, s, $\text{C}(\text{CH}_3)_2\text{Ph}$), 1.64 (3H, s, $\text{C}(\text{CH}_3)_2\text{Ph}$), 1.48 (1H, m, DACH), 1.19 (3H, m, DACH). $^{13}\text{C}\{^1\text{H}\}$ NMR (150 MHz, 25 °C, CDCl_3): δ 163.7, 158.0, 150.8, 150.6, 139.1, 135.8, 128.7, 127.9, 127.7, 127.6, 126.7, 125.6, 125.5, 124.9, 118.1, 69.8, 66.5, 42.4, 42.1, 40.6, 34.9, 31.0, 30.9, 29.7, 29.2, 25.2, 24.6, 23.7. Anal. Calc. for $\text{C}_{33}\text{H}_{42}\text{N}_2\text{O}$: C, 82.11; H, 8.77; N, 5.80. Found: C, 82.02; H, 8.87; N, 5.56.

General procedure for the synthesis of proligands (±) and (*R,R*) $\text{H}(\text{NNO}_R)$. NaCNBH_3 (23 mmol) was added to a solution of the appropriate imine (4.5 mmol) in acetonitrile

(100 mL) and the reaction mixture was stirred for 30 min. Acetic acid (23 mmol) was added dropwise to the solution and it was stirred at room temperature for 18 h. The mixture was diluted with 2% MeOH in DCM (100 mL) and washed with 1M NaOH (3 × 100 mL). The organic layer was dried over MgSO_4 , filtered, and pumped to dryness *in vacuo* to afford the crude compound. The crude compounds were purified using a variety of methods (see below for details). The purified ligands were then stirred in the glovebox under N_2 atmosphere with dry hexane and either filtered (if insoluble) or pumped to dryness (if soluble) to remove trace water and/or methanol impurities before use in metal chemistry.

Synthesis of 2-(((±)-*trans*-2-(dimethylamino)cyclohexylamino)methyl)-4-methyl-6-(triphenylsilyl)phenol (±)- $\text{H}(\text{NNO}_{\text{SiPh}_3})$. The crude product was isolated as an off-white coloured foamy residue. The residue was dissolved in a minimum of hot methanol and the solution was cooled to 0 °C causing precipitation of the pure product, which was isolated via vacuum filtration as an off-white solid and dried under vacuum prior to use (0.227 g, 48 %) ^1H NMR (600 MHz, 25 °C, CDCl_3): δ 7.64 (6H, m, SiPh_3), 7.34 (9H, m, SiPh_3), 6.93 (1H, m, Ar-*H*), 6.82 (1H, m, Ar-*H*), 4.07 (1H, d, $^2J_{\text{HH}} = 12$ Hz, N-*CH*₂-Ar), 3.89 (1H, d, $^2J_{\text{HH}} = 12$ Hz, N-*CH*₂-Ar), 3.35 (1H, m, *NH*), 2.37 (1H, m, *NCH*), 2.17 (6H, s, $\text{N}(\text{CH}_3)_2$), 2.14 (3H, s, Ar-*CH*₃), 2.13 (1H, m, *NCH*), 2.00 (1H, m, DACH), 1.77 (2H, m, DACH), 1.63 (1H, m, DACH), 1.11 (4H, m, DACH). $^{13}\text{C}\{^1\text{H}\}$ NMR (150 MHz, 25 °C, CDCl_3): δ 161.6, 137.1, 136.4, 135.5, 130.9, 128.9, 127.5, 127.1, 123.6, 120.0, 66.5, 59.7, 51.3, 40.0, 31.6, 25.3, 24.7, 20.9, 20.6. Anal. Calc. for $\text{C}_{34}\text{H}_{40}\text{N}_2\text{OSi}$: C, 78.41; H, 7.74; N, 5.38. Found: C, 78.17; H, 7.50; N, 5.21.

Synthesis of 2-(((*R,R*)-*trans*-2-(dimethylamino)cyclohexylamino)methyl)-4-methyl-6-(triphenylsilyl)phenol (*R,R*)- $\text{H}(\text{NNO}_{\text{SiPh}_3})$. The crude product was isolated as an off-white coloured foamy residue. The residue was dissolved in a minimum of hot methanol and the solution was cooled to 0 °C causing precipitation of the pure product, which was isolated via vacuum filtration as a pale off-white solid and dried under vacuum prior to use (0.293 g, 58 %) ^1H NMR (600 MHz, 25 °C, CDCl_3): δ 7.65 (6H, m, SiPh_3), 7.34 (9H, m, SiPh_3), 6.93 (1H, m, Ar-*H*), 6.83 (1H, m, Ar-*H*), 4.07 (1H, d, $^2J_{\text{HH}} = 12$ Hz, N-*CH*₂-Ar), 3.90 (1H, d, $^2J_{\text{HH}} = 18$ Hz, N-*CH*₂-Ar), 3.36 (1H, m, *NH*), 2.37 (1H, m, *NCH*), 2.17 (6H, s, $\text{N}(\text{CH}_3)_2$), 2.15 (3H, s, Ar-*CH*₃), 2.14 (1H, m, *NCH*), 2.01 (1H, m, DACH), 1.77 (2H, m, DACH), 1.64 (1H, m, DACH), 1.12 (4H, m, DACH). $^{13}\text{C}\{^1\text{H}\}$ NMR (150 MHz, 25 °C, CDCl_3): δ 161.6, 137.2, 136.4, 135.5, 131.0, 129.0, 127.5, 127.2, 123.6, 120.0, 66.4, 59.6, 51.2, 40.0, 31.5, 25.3, 24.7, 20.9, 20.6. Anal. Calc. for $\text{C}_{34}\text{H}_{40}\text{N}_2\text{OSi}$: C, 78.41; H, 7.74; N, 5.38. Found: C, 78.09; H, 7.94; N, 5.22.

Synthesis of 2-(((±)-*trans*-2-(dimethylamino)cyclohexylamino)methyl)-4-*t*-butyl-6-(adamantan-1-yl)phenol (±)- $\text{H}(\text{NNO}_{\text{Ad}})$. The crude compound was isolated

as an off-white oily residue. The residue was dissolved in a minimum of hot acetonitrile and the solution was cooled to 0 °C causing precipitation of the pure product, which was isolated by vacuum filtration as an off-white solid and dried under vacuum prior to use (0.365 g, 41 %). ¹H NMR (600 MHz, 25 °C, CDCl₃): δ 7.16 (1H, m, Ar-*H*), 6.89 (1H, m, Ar-*H*), 4.06 (1H, d, ²J_{HH} = 12 Hz, N-CH₂-Ar), 3.72 (1H, d, ²J_{HH} = 12 Hz, N-CH₂-Ar), 2.36 (1H, m, NCH), 2.30 (1H, m, NCH), 2.20 (6H, s, N(CH₃)₂), 2.18 (6H, m, Ad), 2.08 (3H, m, Ad), 1.78 (9H, m, Ad + DACH), 1.63 (1H, m, DACH), 1.30 (9H, s, C(CH₃)₃), 1.21 (4H, m, DACH). ¹³C{¹H} NMR (150 MHz, 25 °C, CDCl₃): δ 154.9, 140.2, 136.2, 123.5, 122.7, 122.5, 66.6, 58.7, 51.4, 40.5, 40.0, 37.2, 37.0, 34.2, 31.7, 29.7, 29.2, 25.4, 24.7, 20.9. Anal. Calc. for C₂₉H₄₆N₂O: C, 79.40; H, 10.57; N, 6.39. Found: C, 79.51; H, 10.96; N, 6.10.

Synthesis of 2-(((*R,R*)-*trans*-2-(dimethylamino)cyclohexylamino)methyl)-4-*t*-butyl-6-(adamantan-1-yl)phenol (*R,R*)-H(NNO_{Ad}). The crude compound was isolated as a pale yellow oily residue. The residue was dissolved in a minimum of hot acetonitrile with a small amount DCM added to fully dissolve the oil. The solution was cooled to 0 °C causing precipitation of the pure product, which was isolated by vacuum filtration as an off-white solid and dried under vacuum prior to use (0.924 g, 40 %). ¹H NMR (600 MHz, 25 °C, CDCl₃): δ 7.17 (1H, m, Ar-*H*), 6.90 (1H, m, Ar-*H*), 4.07 (1H, d, ²J_{HH} = 12 Hz, N-CH₂-Ar), 3.73 (1H, d, ²J_{HH} = 12 Hz, N-CH₂-Ar), 3.38 (1H, m, NH), 2.37 (1H, m, NCH), 2.29 (1H, m, NCH), 2.21 (6H, s, N(CH₃)₂), 2.19 (6H, m, Ad), 2.09 (3H, m, Ad), 1.82 (9H, m, Ad + DACH), 1.72 (1H, m, DACH), 1.31 (9H, s, C(CH₃)₃), 1.22 (4H, m, DACH). ¹³C{¹H} NMR (150 MHz, 25 °C, CDCl₃): δ 155.0, 140.1, 136.2, 123.6, 122.6, 122.5, 66.6, 58.7, 51.4, 40.4, 40.0, 37.2, 37.0, 34.2, 31.7, 29.2, 25.4, 24.7, 20.9. Anal. Calc. for C₂₉H₄₆N₂O: C, 79.40; H, 10.57; N, 6.39. Found: C, 79.24; H, 10.81; N, 6.27.

Synthesis of 2-(((±)-*trans*-2-(dimethylamino)cyclohexylamino)methyl)-4,6-bis(2-phenylpropan-2-yl)phenol (±)-H(NNO_{Cm}). The crude product was isolated as an off-white foamy residue. The residue was dissolved in a minimum of hot methanol and the solution was cooled to 0 °C causing crystallization of the pure product, which was isolated via vacuum filtration as off-white crystals and dried under vacuum prior to use (0.752 g, 65 %). ¹H NMR (600 MHz, 25 °C, CDCl₃): δ 7.28 (4H, m, C(CH₃)₂Ph), 7.19 (6H, m, Ar-*H* + C(CH₃)₂Ph), 7.12 (1H, m, C(CH₃)₂Ph), 6.76 (1H, m, Ar-*H*), 3.81 (2H, m, N-CH₂-Ar), 3.18 (1H, m, NH), 2.26 (1H, m, NCH), 2.14 (6H, s, N(CH₃)₂), 2.13 (1H, m, NCH), 1.89 (1H, m, DACH), 1.74 (2H, m, DACH), 1.70 (9H, s, C(CH₃)₂Ph), 1.66 (3H, s, C(CH₃)₂Ph), 1.60 (1H, m, DACH), 1.09 (3H, m, DACH), 0.98 (1H, m, DACH). ¹³C{¹H} NMR (150 MHz, 25 °C, CDCl₃): δ 154.5, 151.5, 151.4, 139.3, 135.0, 127.8, 127.6, 126.8, 125.7, 125.3, 124.7, 124.6, 123.8, 66.3, 59.1, 51.5, 42.4, 42.1, 40.0, 31.5, 31.0, 30.0, 29.2, 25.2, 24.6, 20.8. Anal. Calc. for C₃₃H₄₄N₂O: C, 81.77; H, 9.15; N, 5.78. Found: C, 81.48; H, 9.41; N, 5.67.

Synthesis of 2-(((*R,R*)-*trans*-2-(dimethylamino)cyclohexylamino)methyl)-4,6-bis(2-phenylpropan-2-yl)phenol (*R,R*)-H(NNO_{Cm}). The crude product was isolated as a thick, yellow coloured oil. The oil was washed with petroleum ether several times, decanting the supernatant solution each time, until no more oil appeared to dissolve. The supernatant petroleum ether solutions were combined together and pumped to dryness *in vacuo* yielding the desired product as a thick, off-white coloured oil (2.71 g, 54%). ¹H NMR (600 MHz, 25 °C, CDCl₃): δ 7.28 (4H, m, C(CH₃)₂Ph), 7.17 (6H, m, Ar-*H* + C(CH₃)₂Ph), 7.11 (1H, m, C(CH₃)₂Ph), 6.74 (1H, m, Ar-*H*), 3.80 (2H, m, N-CH₂-Ar), 2.25 (1H, m, NCH), 2.12 (6H, s, N(CH₃)₂), 2.09 (1H, m, NCH), 1.87 (1H, m, DACH), 1.72 (2H, m, DACH), 1.68 (9H, s, C(CH₃)₂Ph), 1.65 (3H, s, C(CH₃)₂Ph), 1.58 (1H, m, DACH), 1.08 (3H, m, DACH), 0.96 (1H, m, DACH). ¹³C{¹H} NMR (150 MHz, 25 °C, CDCl₃): δ 154.5, 151.5, 151.4, 139.3, 135.0, 127.8, 127.6, 126.7, 125.7, 125.3, 124.7, 124.5, 123.8, 66.3, 59.1, 51.4, 42.4, 42.1, 40.0, 31.5, 31.0, 29.9, 29.2, 25.2, 24.6, 20.8. Anal. Calc. for C₃₃H₄₄N₂O: C, 81.77; H, 9.15; N, 5.78. Found: C, 81.61; H, 9.15; N, 5.43.

General procedure for the synthesis of indium dichloride complexes (±) and (*R,R*) (NNO_R)InCl₂. Potassium *t*-butoxide (0.040 mmol) was transferred using toluene (5 mL) to a solution of the appropriate proligand (±)- or (*R,R*)- H(NNO_R) (0.040 mmol) in toluene (5 mL). This solution was stirred at room temperature for 16 h, and the solvent was removed *in vacuo* yielding (±)- or (*R,R*)- K(NNO_R) in quantitative yield. The potassium salt (±)- or (*R,R*)- K(NNO_R) (0.040 mmol) was dissolved in THF (5 mL). Indium trichloride (0.040 mmol) was transferred to this solution using THF (5 mL). The mixture was stirred at room temperature for 18 h, then filtered through glass fibre filter paper and pumped to dryness *in vacuo* to obtain the crude compound. The crude compounds were purified by a variety of methods depending on the proligand used (see below for details).

Synthesis of complex (±)-1. The crude complex was isolated as a white foamy residue. Acetonitrile was added to the residue and the solution was stirred for several minutes causing precipitation of a white solid. The solution was filtered on a glass frit and a white powder was collected and stirred with ether for approximately 30 min. The solution was pumped to dryness *in vacuo* yielding the desired compound as a white solid in approximately 90 % purity as determined by ¹H NMR spectroscopy (0.2008 g, 79 %). Attempts at further purification were unsuccessful. Single crystals of complex (±)-1 were grown by slow diffusion of hexane into a saturated solution of the complex in THF at room temperature and were analysed by single crystal X-ray diffraction. ¹H NMR (600 MHz, 25 °C, CD₂Cl₂): δ 7.63 (6H, m, SiPh₃), 7.31 (9H, m, SiPh₃), 7.04 (1H, m, Ar-*H*), 6.83 (1H, m, Ar-*H*), 5.02 (1H, d, ²J_{HH} = 12 Hz, CH₂N), 3.78 (1H, d, ²J_{HH} = 12 Hz, CH₂N), 2.94 (1H, m, NH), 2.74 (1H, m, CHN), 2.54 (1H, m, CHN), 2.44 (1H, m, DACH), 2.38 (3H,

s, NCH_3), 2.12 (3H, s, NCH_3), 1.83 (3H, m, DACH), 1.27 (1H, m, DACH), 1.20 (2H, m, DACH), 1.12 (3H, s, Ar- CH_3), 0.98 (1H, m, DACH). $^{13}\text{C}\{^1\text{H}\}$ NMR (151 MHz, 25 °C, CD_2Cl_2): δ 169.3, 139.7, 137.5, 137.3, 136.8, 135.0, 129.1, 127.8, 127.8, 124.8, 124.7, 118.8, 65.8, 50.5, 44.2, 37.1, 31.1, 25.1, 25.0, 22.2, 20.6. Anal. Calc. for $\text{C}_{34}\text{H}_{39}\text{Cl}_2\text{InN}_2\text{OSi}$: C, 57.88; H, 5.57; N, 3.97. Found: C, 58.30; H, 5.68; N, 4.79.

Synthesis of complex (R,R)-1. The crude complex was obtained as an off-white foamy residue. Acetonitrile was added to this residue and the solution was stirred for several minutes causing precipitation of an off-white solid. The solution was filtered on a glass frit and an off-white solid was collected and stirred with ether for approximately 30 min. The solution was pumped to dryness *in vacuo* yielding the desired compound as an off-white solid in approximately 90 % purity as determined by ^1H NMR spectroscopy (0.1246 g, 57 %). Attempts at further purification were unsuccessful. ^1H NMR (600 MHz, 25 °C, CD_2Cl_2): δ 7.64 (6H, m, SiPh₃), 7.31 (9H, m, SiPh₃), 7.07 (1H, m, ArH), 6.87 (1H, m, ArH), 5.16 (1H, d, $^2J_{\text{HH}} = 18$ Hz, CH_2N), 3.80 (1H, d, $^2J_{\text{HH}} = 12$ Hz, CH_2N), 2.96 (1H, m, NH), 2.67 (1H, m, CHN), 2.54 (1H, m, CHN), 2.45 (1H, m, DACH), 2.33 (3H, s, NCH_3), 2.15 (3H, s, NCH_3), 1.78 (3H, m, DACH), 1.17 (3H, m, DACH), 1.05 (3H, s, Ar- CH_3), 0.95 (1H, m, DACH). $^{13}\text{C}\{^1\text{H}\}$ NMR (151 MHz, 25 °C, CD_2Cl_2): δ 169.4, 139.6, 137.6, 137.3, 136.8, 135.2, 129.1, 127.8, 127.8, 124.9, 124.7, 118.9, 65.6, 53.8, 50.5, 44.1, 37.0, 31.2, 25.1, 25.0, 22.1, 20.6. Anal. Calc. for $\text{C}_{34}\text{H}_{39}\text{Cl}_2\text{InN}_2\text{OSi}$: C, 57.88; H, 5.57; N, 3.97. Found: C, 57.70; H, 5.50; N, 4.04.

Synthesis of complex (\pm)-2. The crude complex was isolated as a yellow, foamy residue. Toluene was added until the residue just dissolved (1-3 mL), then hexane was added until a precipitate just began to form (2-5 mL). The solution was left in the freezer (-35 °C) overnight, causing the precipitation of a pale yellow solid. The solution was filtered on a glass frit yielding the purified complex as a pale yellow powder, which was dried under vacuum prior to use (0.2518 g, 80 %). Single crystals of complex (\pm)-2 were grown from a saturated solution of the complex in toluene at room temperature and were analysed by single crystal X-ray diffraction. ^1H NMR (600 MHz, 25 °C, CD_2Cl_2): δ 7.17 (1H, m, Ar-H), 6.84 (1H, m, Ar-H), 4.43 (1H, m, N- CH_2 -Ar), 4.00 (1H, m, N- CH_2 -Ar), 2.76 (1H, m, NCH), 2.72 (3H, s, $\text{N}(\text{CH}_3)_2$), 2.56 (2H, m, NCH + NH), 2.42 (1H, m, DACH), 2.29 (3H, s, $\text{N}(\text{CH}_3)_2$), 2.22 (3H, m, Ad), 2.17 (3H, m, Ad), 2.03 (3H, m, Ad), 2.00 (1H, m, DACH), 1.89 (2H, m, DACH), 1.83 (3H, m, Ad), 1.75 (3H, m, Ad), 1.34 (1H, m, DACH), 1.28 (9H, s, $\text{C}(\text{CH}_3)_3$), 1.22 (3H, m, DACH). $^{13}\text{C}\{^1\text{H}\}$ NMR (151 MHz, 25 °C, CD_2Cl_2): δ 161.8, 140.1, 138.7, 125.5, 124.9, 121.2, 66.3, 55.2, 51.9, 44.7, 41.0, 38.3, 37.9, 37.7, 34.5, 32.0, 31.6, 30.0, 25.0, 25.0, 22.5. Anal. Calc. for $\text{C}_{29}\text{H}_{45}\text{Cl}_2\text{InN}_2\text{O}$: C, 55.87; H, 7.28; N, 4.49. Found: C, 56.16; H, 7.27; N, 4.51.

Synthesis of complex (R,R)-2. The crude complex was isolated as a yellow residue. The residue was dissolved in a

minimum of ether, then hexane was added causing precipitation of a yellow solid. The supernatant solution was removed and the resulting solid was washed 2x with more hexane. The solid was dried under vacuum yielding the purified complex as a pale yellow powder in approximately 90 % purity as determined by ^1H NMR spectroscopy (0.0213 g, 30 %). Attempts at further purification were not successful and therefore elemental analysis of this complex was not pursued. ^1H NMR (600 MHz, 25 °C, CD_2Cl_2): δ 7.19 (1H, m, Ar-H), 6.88 (1H, m, Ar-H), 4.16 (1H, m, N- CH_2 -Ar), 4.10 (1H, m, N- CH_2 -Ar), 2.74 (3H, s, $\text{N}(\text{CH}_3)_2$), 2.66 (1H, m, NCH), 2.59 (2H, m, NCH + NH), 2.43 (3H, s, $\text{N}(\text{CH}_3)_2$), 2.21 (4H, m, DACH + Ad), 2.17 (3H, m, Ad), 2.09 (1H, m, DACH), 2.04 (3H, m, Ad), 1.90 (1H, m, DACH), 1.88 (1H, m, DACH), 1.83 (3H, m, Ad), 1.75 (3H, m, Ad), 1.34 (1H, m, DACH), 1.28 (9H, s, $\text{C}(\text{CH}_3)_3$), 1.20 (3H, m, DACH). $^{13}\text{C}\{^1\text{H}\}$ NMR (151 MHz, 25 °C, CD_2Cl_2): δ 161.4, 140.5, 139.3, 125.1, 121.9, 66.8, 55.9, 52.3, 44.7, 41.0, 38.1, 37.9, 37.7, 34.6, 32.0, 31.9, 30.0, 25.0, 25.0, 22.5.

Synthesis of complex (\pm)-3

The crude complex was isolated as a pale off-white residue. This residue was stirred with ether for approximately 30 min, causing the precipitation of a white solid. This solution was filtered on a glass frit yielding the pure complex as a white powder, which was dried under vacuum prior to use (0.2459 g, 88 %). ^1H NMR spectroscopy confirmed the presence of small unknown impurities in the purified complex, however attempts at further purification were unsuccessful. ^1H NMR (600 MHz, 25 °C, CD_2Cl_2): δ 7.31 (1H, m, Ar-H), 7.27 (4H, m, $\text{C}(\text{CH}_3)_2\text{Ph}$), 7.24 (2H, m, $\text{C}(\text{CH}_3)_2\text{Ph}$), 7.16 (3H, m, $\text{C}(\text{CH}_3)_2\text{Ph}$), 7.03 (1H, m, $\text{C}(\text{CH}_3)_2\text{Ph}$), 6.69 (1H, m, Ar-H), 4.35 (1H, d, $^2J_{\text{HH}} = 12$ Hz, N- CH_2 -Ar), 3.84 (1H, m, N- CH_2 -Ar), 2.63 (1H, m, NCH), 2.54 (3H, s, $\text{N}(\text{CH}_3)_2$), 2.40 (2H, m, NCH + DACH), 2.34 (1H, m, NH), 1.91 (1H, m, DACH), 1.84 (1H, m, DACH), 1.78 (4H, m, $\text{C}(\text{CH}_3)_2\text{Ph}$ + DACH), 1.73 (3H, s, $\text{N}(\text{CH}_3)_2$), 1.68 (3H, s, $\text{C}(\text{CH}_3)_2\text{Ph}$), 1.67 (3H, s, $\text{C}(\text{CH}_3)_2\text{Ph}$), 1.57 (3H, s, $\text{C}(\text{CH}_3)_2\text{Ph}$), 1.27 (1H, m, DACH), 1.11 (3H, m, DACH). $^{13}\text{C}\{^1\text{H}\}$ NMR (151 MHz, 25 °C, CD_2Cl_2): δ 161.4, 152.3, 151.6, 139.1, 137.6, 128.3, 128.0, 128.0, 127.2, 127.2, 126.9, 125.8, 125.1, 120.9, 66.0, 55.0, 51.5, 44.4, 42.7, 42.5, 37.5, 31.7, 31.4, 31.3, 31.3, 27.8, 24.9, 22.4. Anal. Calc. for $\text{C}_{33}\text{H}_{43}\text{Cl}_2\text{InN}_2\text{O}$: C, 59.21; H, 6.47; N, 4.18. Found: C, 59.36; H, 6.51; N, 4.96.

Synthesis of complex (R,R)-3. The crude complex was isolated as a pale yellow, foamy solid. The solid was dissolved in a minimum of ether then hexane was added causing precipitation of a small amount of off-white solid, which was filtered on a glass frit. The filtrate was pumped to dryness and this process was repeated, yielding a second portion of the product. The solids were combined and dried under vacuum yielding an off-white solid (0.3198 g, 74 %). The ^1H NMR spectrum of the solid showed a mixture of the desired complex and a significant amount of unknown impurities. A small amount of pure complex was obtained by precipitation from a saturated solution of this crude complex in hexane, however

large-scale purification using this method was not successful and purification and full characterization of this complex was not pursued further. ^1H NMR (600 MHz, 25 °C, CD_2Cl_2): δ 7.32 (1H, m, Ar-H), 7.28 (4H, m, $\text{C}(\text{CH}_3)_2\text{Ph}$), 7.21 (2H, m, $\text{C}(\text{CH}_3)_2\text{Ph}$), 7.16 (3H, m, $\text{C}(\text{CH}_3)_2\text{Ph}$), 7.04 (1H, m, $\text{C}(\text{CH}_3)_2\text{Ph}$), 6.74 (1H, m, Ar-H), 4.02 (1H, m, N- CH_2 -Ar), 3.96 (1H, m, N- CH_2 -Ar), 2.63 (3H, s, $\text{N}(\text{CH}_3)_2$), 2.55 (1H, m, NCH), 2.42 (2H, m, NCH + DACH), 2.16 (3H, s, $\text{N}(\text{CH}_3)_2$), 2.00 (2H, m, NH + DACH), 1.88 (1H, m, DACH), 1.81 (1H, m, DACH), 1.75 (3H, m, $\text{C}(\text{CH}_3)_2\text{Ph}$), 1.68 (3H, s, $\text{C}(\text{CH}_3)_2\text{Ph}$), 1.67 (3H, s, $\text{C}(\text{CH}_3)_2\text{Ph}$), 1.60 (3H, s, $\text{C}(\text{CH}_3)_2\text{Ph}$), 1.27 (1H, m, DACH), 1.11 (3H, m, DACH). $^{13}\text{C}\{^1\text{H}\}$ NMR (151 MHz, 25 °C, CD_2Cl_2): δ 160.88, 152.1, 151.7, 139.8, 138.2, 128.4, 128.0, 127.5, 127.3, 127.1, 127.0, 125.9, 125.1, 121.8, 66.5, 55.9, 52.0, 44.5, 42.8, 42.5, 37.8, 31.7, 31.3, 31.3, 31.1, 28.6, 25.0, 24.9, 22.5.

General procedure for the synthesis of indium ethoxide complexes (\pm) and (*R,R*) $[(\text{NNO}_R)\text{InCl}_2(\mu\text{-Cl})(\mu\text{-OEt})]$. Toluene (5 mL) was used to transfer sodium ethoxide (0.1394 mmol) to a solution of the appropriate indium dichloride complex (0.1422 mmol) in toluene (5 mL). The solution was stirred at room temperature for ~ 18 h, then the mixture was filtered through glass fibre filter paper and purified by a variety of methods depending on the dichloride used (see below for details).

Synthesis of complex (\pm)-4. The filtered crude reaction mixture was concentrated *in vacuo* until a white precipitate just began to form (1-2 mL). Ether (~ 5 mL) was then added and the solution was stirred for several minutes. The solution was filtered on a glass frit yielding a white solid. The solid was collected and stirred with ether for approximately 30 min, then pumped to dryness for several hours to remove residual solvents. This yielded the purified complex as a white solid (0.0306 g, 58 %). ^1H NMR spectroscopy confirmed the presence of small unknown impurities in the purified complex, however attempts at further purification were unsuccessful. ^1H NMR (600 MHz, 25 °C, CDCl_3): δ 7.71 (6H, m, SiPh_3), 7.32 (9H, m, SiPh_3), 7.24 (1H, m, ArH), 6.80 (1H, m, ArH), 4.92 (1H, d, $^2J_{\text{HH}} = 12$ Hz, CH_2N), 3.93 (1H, m, OCH_2CH_3), 3.64 (1H, d, $^2J_{\text{HH}} = 12$ Hz, CH_2N), 2.84 (1H, m, NH), 2.76 (1H, m, CHN), 2.37 (2H, m, CHN + DACH), 2.30 (3H, s, NCH_3), 2.17 (3H, s, NCH_3), 1.75 (3H, m, DACH), 1.13 (4H, m, DACH), 0.92 (3H, s, Ar- CH_3), 0.84 (1.5H, t, $^3J_{\text{HH}} = 12$ Hz, OCH_2CH_3). $^{13}\text{C}\{^1\text{H}\}$ NMR (151 MHz, 25 °C, CDCl_3): δ 165.5, 139.9, 137.0, 136.8, 136.1, 135.3, 128.4, 127.4, 127.2, 124.2, 123.5, 118.9, 64.2, 62.6, 52.6, 50.2, 43.6, 36.5, 30.6, 24.7, 24.6, 21.5, 20.4, 19.7. Anal. Calc. for $\text{C}_{70}\text{H}_{83}\text{Cl}_3\text{In}_2\text{N}_4\text{O}_3\text{Si}_2$: C, 59.18; H, 5.89; N, 3.94. Found: C, 58.84; H, 5.99; N, 4.07.

Synthesis of complex (*R,R*)-4. The crude complex was isolated as a clear, colourless oily residue. The residue was dissolved in a minimum of toluene, then hexane was added until a white solid precipitated out of solution. The supernatant solution was removed, then the solid was washed 2x with more

hexane. The solid was dried under vacuum yielding the purified complex as a white solid (0.0532 g, 42 %). ^1H NMR spectroscopy confirmed the presence of small unknown impurities in the purified complex, however attempts at further purification were unsuccessful. ^1H NMR (600 MHz, 25 °C, CDCl_3): δ 7.70 (6H, m, SiPh_3), 7.32 (9H, m, SiPh_3), 7.24 (1H, m, ArH), 6.79 (1H, m, ArH), 4.92 (1H, d, $^2J_{\text{HH}} = 12$ Hz, CH_2N), 3.93 (1H, m, OCH_2CH_3), 3.64 (1H, d, $^2J_{\text{HH}} = 12$ Hz, CH_2N), 2.83 (1H, m, NH), 2.76 (1H, m, CHN), 2.36 (2H, m, CHN + DACH), 2.30 (3H, s, NCH_3), 2.16 (3H, s, NCH_3), 1.75 (3H, m, DACH), 1.13 (4H, m, DACH), 0.91 (3H, s, Ar- CH_3), 0.84 (1.5H, t, $^3J_{\text{HH}} = 12$ Hz, OCH_2CH_3). $^{13}\text{C}\{^1\text{H}\}$ NMR (151 MHz, 25 °C, CDCl_3): δ 165.5, 139.9, 137.0, 136.1, 135.3, 128.4, 127.4, 124.2, 123.5, 118.9, 64.2, 62.6, 52.6, 50.2, 43.6, 36.5, 30.6, 24.8, 24.6, 21.5, 20.4, 19.7. Anal. Calc. for $\text{C}_{70}\text{H}_{83}\text{Cl}_3\text{In}_2\text{N}_4\text{O}_3\text{Si}_2$: C, 59.18; H, 5.89; N, 3.94. Found: C, 59.41; H, 5.97; N, 3.99.

Synthesis of complex (\pm)-5. The crude complex was isolated as a pale yellow residue. The residue was dissolved in ether (1-2 mL) and hexane was added until a pale yellow precipitate began to form (~ 5 mL). The solution was concentrated *in vacuo* to < 2 mL volume, then more hexane (1-2 mL) was added causing precipitation of more solid. This process was repeated 1 more time, yielding a cloudy pale yellow solution, which was filtered on a glass frit. The resulting pale yellow solid was collected and dried under vacuum. The filtrate was dissolved in ether (1-2 mL) and hexane was added (~ 5 mL). This solution was filtered a second time yielding more pale yellow solid, which was combined with the first batch and dried under vacuum several hours to yield the purified complex as a pale yellow solid (0.0603 g, 42 %). Single crystals of complex (\pm)-5 were grown from a saturated solution of the complex in acetonitrile at room temperature and were analysed by single crystal X-ray diffraction. ^1H NMR (600 MHz, 25 °C, CDCl_3): δ 7.14 (1H, m, Ar-H), 6.73 (1H, m, Ar-H), 4.99 (1H, d, $^2J_{\text{HH}} = 12$ Hz, N- CH_2 -Ar), 4.48 (0.5H, m, - OCH_2CH_3), 4.40 (0.5H, m, - OCH_2CH_3), 3.74 (1H, d, $^2J_{\text{HH}} = 12$ Hz, N- CH_2 -Ar), 2.84 (1H, m, NCH), 2.77 (1H, m, NCH), 2.69 (3H, s, $\text{N}(\text{CH}_3)_2$), 2.56 (1H, m, DACH), 2.48 (1H, m, NH), 2.27 (3H, m, Ad), 2.18 (3H, m, Ad), 2.03 (3H, s, Ad), 2.02 (3H, s, $\text{N}(\text{CH}_3)_2$), 1.91 (1H, m, DACH), 1.86 (2H, m, DACH), 1.82 (3H, m, Ad), 1.73 (3H, m, Ad), 1.32 (1.5H, t, $^3J_{\text{HH}} = 6$ Hz, - OCH_2CH_3), 1.28 (9H, s, $\text{C}(\text{CH}_3)_3$), 1.25 (2H, m, DACH), 1.13 (1H, m, DACH), 1.03 (1H, m, DACH). $^{13}\text{C}\{^1\text{H}\}$ NMR (151 MHz, 25 °C, CDCl_3): δ 162.5, 139.0, 136.4, 125.7, 123.8, 118.7, 64.6, 62.8, 52.6, 50.8, 44.2, 40.5, 38.1, 37.4, 37.4, 33.9, 31.8, 30.8, 29.4, 24.8, 24.7, 21.9, 19.5. Anal. Calc. for $\text{C}_{60}\text{H}_{95}\text{Cl}_3\text{In}_2\text{N}_4\text{O}_3$: C, 57.36; H, 7.62; N, 4.46. Found: C, 57.37; H, 7.52; N, 4.47.

Synthesis of complex (*R,R*)-5. The crude reaction mixture was filtered and pumped to dryness *in vacuo* yielding a pale yellow foamy solid. This solid was stirred in ether for approximately 30 min, then pumped to dryness *in vacuo* yielding the product as a pale yellow foamy solid (0.0483 g, 44 %). Due to the high solubility of this compound in all common organic solvents it

was used without further purification. ^1H NMR (600 MHz, 25 °C, CDCl_3): δ 7.13 (1H, m, Ar-*H*), 6.72 (1H, m, Ar-*H*), 4.99 (1H, d, $^2J_{\text{HH}} = 12$ Hz, N- CH_2 -Ar), 4.48 (0.5H, m, - OCH_2CH_3), 4.40 (0.5H, m, - OCH_2CH_3), 3.74 (1H, d, $^2J_{\text{HH}} = 12$ Hz, N- CH_2 -Ar), 2.84 (1H, m, NCH), 2.77 (1H, m, NCH), 2.69 (3H, s, N(CH_3) $_2$), 2.57 (1H, m, DACH), 2.48 (1H, m, NH), 2.27 (3H, m, Ad), 2.18 (3H, m, Ad), 2.03 (3H, s, Ad), 2.02 (3H, s, N(CH_3) $_2$), 1.91 (1H, m, DACH), 1.86 (2H, m, DACH), 1.82 (3H, m, Ad), 1.73 (3H, m, Ad), 1.32 (1.5H, t, $^3J_{\text{HH}} = 6$ Hz, - OCH_2CH_3), 1.28 (9H, s, C(CH_3) $_3$), 1.25 (2H, m, DACH), 1.13 (1H, m, DACH), 1.03 (1H, m, DACH). $^{13}\text{C}\{^1\text{H}\}$ NMR (151 MHz, 25 °C, CDCl_3): δ 162.5, 139.0, 136.3, 125.7, 123.8, 118.7, 64.6, 62.8, 52.6, 50.8, 44.2, 40.5, 38.1, 37.4, 37.4, 33.9, 31.8, 30.8, 29.4, 24.8, 24.7, 21.9, 19.5. Anal. Calc. for $\text{C}_{60}\text{H}_{95}\text{Cl}_3\text{In}_2\text{N}_4\text{O}_3$: C, 57.36; H, 7.62; N, 4.46. Found: C, 54.82; H, 7.29; N, 4.93.

Synthesis of complex (\pm)-6. The crude complex was isolated as a clear, colourless residue. This residue was stirred with hexane for approximately 30 min, causing the precipitation of a white solid. The solution was filtered yielding the purified complex as a white powder, which was dried under vacuum prior to use (0.0402 g, 78 %). Single crystals of complex (\pm)-6 were grown from a saturated solution of the complex in toluene at room temperature and were analysed by single crystal X-ray diffraction. ^1H NMR (600 MHz, 25 °C, CDCl_3): δ 7.37 (1H, m, Ar-*H*), 7.26 (6H, m, C(CH_3) $_2$ Ph), 7.15 (3H, m, C(CH_3) $_2$ Ph), 6.99 (1H, m, C(CH_3) $_2$ Ph), 6.55 (1H, m, Ar-*H*), 4.82 (1H, d, $^2J_{\text{HH}} = 12$ Hz, N- CH_2 -Ar), 3.99 (0.5H, m, - OCH_2CH_3), 3.81 (0.5H, m, - OCH_2CH_3), 3.55 (1H, d, $^2J_{\text{HH}} = 12$ Hz, N- CH_2 -Ar), 2.66 (1H, m, NCH), 2.59 (1H, m, NCH), 2.42 (3H, s, N(CH_3) $_2$), 2.27 (2H, m, NH + DACH), 1.78 (3H, s, C(CH_3) $_2$ Ph), 1.74 (3H, m, DACH), 1.72 (3H, s, C(CH_3) $_2$ Ph), 1.70 (3H, s, C(CH_3) $_2$ Ph), 1.64 (3H, s, C(CH_3) $_2$ Ph), 1.16 (1H, m, DACH), 1.15 (3H, s, N(CH_3) $_2$), 1.05 (1H, m, DACH), 0.96 (1H, m, DACH), 0.90 (1.5H, m, - OCH_2CH_3), 0.85 (1H, m, DACH). $^{13}\text{C}\{^1\text{H}\}$ NMR (151 MHz, 25 °C, CDCl_3): δ 161.9, 152.3, 151.2, 138.1, 135.2, 128.8, 127.7, 127.3, 126.9, 126.7, 125.7, 125.1, 124.1, 118.7, 64.3, 62.6, 52.4, 50.4, 43.8, 42.2, 42.0, 36.5, 31.1, 31.0, 31.0, 30.5, 27.6, 24.7, 24.5, 21.7, 19.2. Anal. Calc. for $\text{C}_{68}\text{H}_{91}\text{Cl}_3\text{In}_2\text{N}_4\text{O}_3$: C, 60.57; H, 6.80; N, 4.15. Found: C, 60.66; H, 6.99; N, 4.03.

Determination of the kinetics of *rac*, L and D lactide polymerization. Three stock solutions of *rac*, L and D lactide (960 mM) and an internal standard 1,3,5-trimethoxybenzene (60 mM) were made in 1 mL volumetric flasks in CDCl_3 and 0.5 mL of each solution was syringed into three separate Teflon-sealed NMR tubes and frozen using a liquid N_2 cold well. Next, a buffer layer of CDCl_3 (0.25 mL) was added to each tube and frozen using the liquid N_2 cold well. Then, a catalyst stock solution (9.6 mM) was made in a 2 mL volumetric flask in CDCl_3 and 0.25 mL of this solution was syringed into each of the three tubes and frozen using the liquid N_2 cold well. The tubes were quickly evacuated while frozen and sealed under vacuum to remove N_2 from the headspace of

the tube. The tubes were kept frozen in liquid N_2 until use. Each sample was quickly warmed to room temperature and mixed before inserting into the NMR spectrometer (400 MHz Inverse Avance Bruker Spectrometer). The polymerizations were then monitored to over 90 % conversion by ^1H NMR spectroscopy. The delay time between removal of the tube from the liquid N_2 and the first ^1H NMR spectrum taken was measured by stopwatch. While every effort was made to complete the set-up of the experiment within a similar time frame for all samples (typically 5-10 minutes) the fast rates of polymerization for some samples led to the first ^1H NMR experiment being taken at significant conversion of monomer ($t = 0$ up to 30 % conversion for some samples, e.g. for L-LA polymerization). The initiation periods observed in the plots of $\ln([\text{LA}])$ vs. time (see SI, Figures S11-S15) therefore do not represent the whole of the initiation period for these samples and can therefore not be compared between different samples.

Representative large-scale polymerization of *rac*-LA

The appropriate amount of catalyst (e.g. for 500 eq. LA, 0.0028 mmol) was transferred using DCM (~ 3 mL) to a stirring solution of *rac*-LA (0.200 g, 1.39 mmol) in DCM (~ 2 mL). The resulting mixture was stirred overnight at room temperature and a test sample was removed and pumped to dryness, then dissolved in CDCl_3 and analysed by ^1H and $^1\text{H}\{^1\text{H}\}$ NMR spectroscopy to determine conversion and tacticity, respectively. The rest of the reaction mixture was concentrated in air under vacuum to < 1 mL volume, then methanol was added while stirring to precipitate the pure polymer as a white solid. The supernatant solution was removed and the resulting polymer was dissolved in a minimum of DCM (< 1 mL). Again, methanol was added while stirring to precipitate the pure polymer and the supernatant solution was removed. This process was repeated 1 more time and the resulting polymer was washed once with pure methanol, then dried under vacuum overnight at room temperature. The polymer was then dried under vacuum overnight at ~ 50 °C in a vacuum oven and the ^1H NMR spectrum was taken of the dried polymer to confirm that no catalyst or solvent remained before analysis by GPC in THF.

Acknowledgements

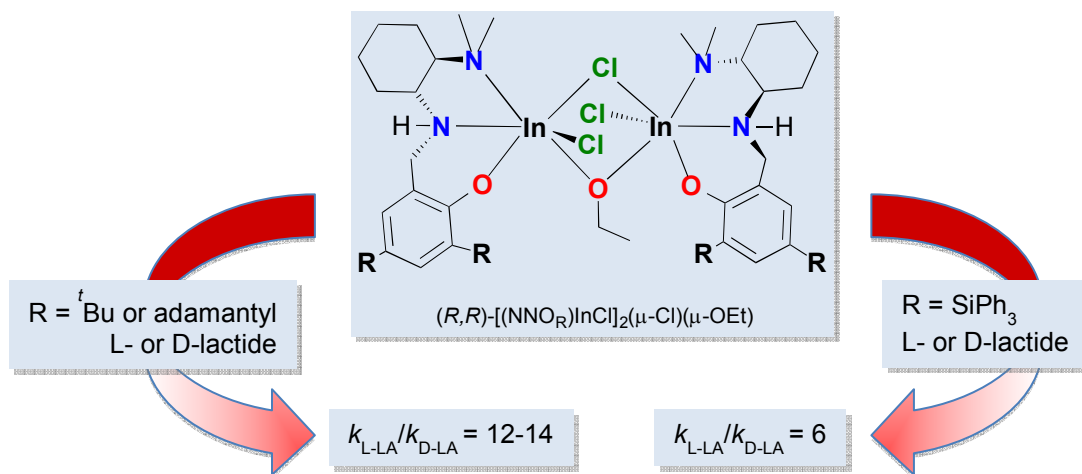
PM gratefully acknowledges support from NSERC Discovery and Strategic grants. KO would like to acknowledge the assistance of Molly Sung for preparation of some ligands.

Notes and references

^a Department of Chemistry, University of British Columbia, 2036 Main Mall, Vancouver, British Columbia V6T 1Z1, Canada.

[†] Electronic Supplementary Information (ESI) available: Associated NMR spectroscopic data and kinetic studies of polymerization (Figures S1-S20) as well as detailed X-ray crystallographic parameters (Table S1) are included. See DOI: 10.1039/b000000x/

1. O. Dechy-Cabaret, B. Martin-Vaca and D. Bourissou, *Chemical Reviews*, 2004, **104**, 6147-6176.
2. R. E. Drumright, P. R. Gruber and D. E. Henton, *Advanced Materials*, 2000, **12**, 1841-1846.
3. B. Gupta, N. Revagade and J. Hilborn, *Progress In Polymer Science*, 2007, **32**, 455-482.
4. J. K. Oh, *Soft Matter*, 2011, **7**, 5096-5108.
5. M. J. Stanford and A. P. Dove, *Chemical Society Reviews*, 2010, **39**, 486-494.
6. C. M. Thomas, *Chemical Society Reviews*, 2010, **39**, 165-173.
7. P. J. Dijkstra, H. Z. Du and J. Feijen, *Polymer Chemistry*, 2011, **2**, 520-527.
8. K. Fukushima and Y. Kimura, *Polymer International*, 2006, **55**, 626-642.
9. N. E. Kamber, W. Jeong, R. M. Waymouth, R. C. Pratt, B. G. G. Lohmeijer and J. L. Hedrick, *Chemical Reviews*, 2007, **107**, 5813-5840.
10. N. Nomura, R. Ishii, M. Akakura and K. Aoi, *Journal of the American Chemical Society*, 2002, **124**, 5938-5939.
11. P. Hornmirun, E. L. Marshall, V. C. Gibson, A. J. P. White and D. J. Williams, *Journal of the American Chemical Society*, 2004, **126**, 2688-2689.
12. R. Ishii, N. Nomura and T. Kondo, *Polymer Journal*, 2004, **36**, 261-264.
13. Z. H. Tang, X. S. Chen, X. Pang, Y. K. Yang, X. F. Zhang and X. B. Jing, *Biomacromolecules*, 2004, **5**, 965-970.
14. Z. H. Tang, X. S. Chen, Y. K. Yang, X. Pang, J. R. Sun, X. F. Zhang and X. B. Jing, *Journal of Polymer Science Part A - Polymer Chemistry*, 2004, **42**, 5974-5982.
15. P. Hornmirun, E. L. Marshall, V. C. Gibson, R. I. Pugh and A. J. P. White, *Proceedings of the National Academy of Sciences of the United States of America*, 2006, **103**, 15343-15348.
16. N. Nomura, R. Ishii, Y. Yamamoto and T. Kondo, *Chemistry - A European Journal*, 2007, **13**, 4433-4451.
17. M. Bouyahyi, E. Grunova, N. Marquet, E. Kirillov, C. M. Thomas, T. Roisnel and J. F. Carpentier, *Organometallics*, 2008, **27**, 5815-5825.
18. A. Alaaeddine, C. M. Thomas, T. Roisnel and J. F. Carpentier, *Organometallics*, 2009, **28**, 1469-1475.
19. M. Bouyahyi, T. Roisnel and J. F. Carpentier, *Organometallics*, 2010, **29**, 491-500.
20. N. Nomura, A. Akita, R. Ishii and M. Mizuno, *Journal of the American Chemical Society*, 2010, **132**, 1750-1751.
21. M. Normand, V. Dorcet, E. Kirillov and J. F. Carpentier, *Organometallics*, 2013, **32**, 1694-1709.
22. N. Spassky, M. Wisniewski, C. Pluta and A. LeBorgne, *Macromolecular Chemistry and Physics*, 1996, **197**, 2627-2637.
23. T. M. Ovitt and G. W. Coates, *Journal of Polymer Science Part A - Polymer Chemistry*, 2000, **38**, 4686-4692.
24. C. P. Radano, G. L. Baker and M. R. Smith, *Journal of the American Chemical Society*, 2000, **122**, 1552-1553.
25. T. M. Ovitt and G. W. Coates, *Journal of the American Chemical Society*, 2002, **124**, 1316-1326.
26. Z. Y. Zhong, P. J. Dijkstra and J. Feijen, *Angewandte Chemie - International Edition*, 2002, **41**, 4510-4513.
27. Z. Y. Zhong, P. J. Dijkstra and J. Feijen, *Journal of the American Chemical Society*, 2003, **125**, 11291-11298.
28. I. P. Hsieh, C. H. Huang, H. M. Lee, P. C. Kuo, J. H. Huang, H. I. Lee, J. T. Cheng and G. H. Lee, *Inorganica Chimica Acta*, 2006, **359**, 497-504.
29. I. Peckermann, A. Kapelski, T. P. Spaniol and J. Okuda, *Inorganic Chemistry*, 2009, **48**, 5526-5534.
30. A. Pietrangelo, M. A. Hillmyer and W. B. Tolman, *Chemical Communications*, 2009, 2736-2737.
31. J.-C. Buffet, J. Okuda and P. L. Arnold, *Inorganic Chemistry*, 2010, **49**, 419-426.
32. M. G. Hu, M. Wang, P. L. Zhang, L. Wang, F. J. Zhu and L. C. Sun, *Inorganic Chemistry Communications*, 2010, **13**, 968-971.
33. A. Pietrangelo, S. C. Knight, A. K. Gupta, L. J. Yao, M. A. Hillmyer and W. B. Tolman, *Journal of the American Chemical Society*, 2010, **132**, 11649-11657.
34. M. P. Blake, A. D. Schwarz and P. Mountford, *Organometallics*, 2011, **30**, 1202-1214.
35. M. Bompard, J. Vergnaud, H. Strub and J. F. Carpentier, *Polymer Chemistry*, 2011, **2**, 1638-1640.
36. E. M. Broderick, N. Guo, C. S. Vogel, C. Xu, J. Sutter, J. T. Miller, K. Meyer, P. Mehrkhodavandi and P. L. Diaconescu, *Journal of the American Chemical Society*, 2011, **133**, 9278-9281.
37. M. Normand, E. Kirillov, T. Roisnel and J. F. Carpentier, *Organometallics*, 2012, **31**, 1448-1457.
38. L. E. N. Allan, G. G. Briand, A. Decken, J. D. Marks, M. P. Shaver and R. G. Wareham, *Journal of Organometallic Chemistry*, 2013, **736**, 55-62.
39. A. Kapelski and J. Okuda, *Journal of Polymer Science Part A - Polymer Chemistry*, 2013, **51**, 4983-4991.
40. N. Maudoux, T. Roisnel, V. Dorcet, J. F. Carpentier and Y. Sarazin, *Chemistry - A European Journal*, 2014, **20**, DOI: 10.1002/chem.201304788.
41. G. Labourdette, D. J. Lee, B. O. Patrick, M. B. Ezhova and P. Mehrkhodavandi, *Organometallics*, 2009, **28**, 1309-1319.
42. D. C. Aluthge, B. O. Patrick and P. Mehrkhodavandi, *Chemical Communications*, 2013, **49**, 4295-4297.
43. D. C. Aluthge, E. X. Yan, J.-M. Ahn and P. Mehrkhodavandi, *Inorganic Chemistry*, 2014, DOI: 10.1021/ic500647j.
44. A. F. Douglas, B. O. Patrick and P. Mehrkhodavandi, *Angewandte Chemie - International Edition*, 2008, **47**, 2290-2293.
45. A. Acosta-Ramirez, A. F. Douglas, I. Yu, B. O. Patrick, P. L. Diaconescu and P. Mehrkhodavandi, *Inorganic Chemistry*, 2010, **49**, 5444-5452.
46. K. M. Osten, I. Yu, I. R. Duffy, P. O. Lagaditis, J. C. C. Yu, C. J. Wallis and P. Mehrkhodavandi, *Dalton Transactions*, 2012, **41**, 8123-8134.
47. C. Xu, I. Yu and P. Mehrkhodavandi, *Chemical Communications*, 2012, **48**, 6806-6808.
48. I. Yu, A. Acosta-Ramirez and P. Mehrkhodavandi, *Journal of the American Chemical Society*, 2012, **134**, 12758-12773.
49. D. C. Aluthge, C. L. Xu, N. Othman, N. Noroozi, S. G. Hatzikiriakos and P. Mehrkhodavandi, *Macromolecules*, 2013, **46**, 3965-3974.
50. K. M. Osten, D. C. Aluthge, B. O. Patrick and P. Mehrkhodavandi, *Inorganic Chemistry*, 2014, **53**, 9897-9906.
51. X. Zhang, T. J. Emge and K. C. Hultsch, *Organometallics*, 2010, **29**, 5871-5877.
52. N. U. Hofsklokken and L. Skattebol, *Acta Chemica Scandinavica*, 1999, **53**, 258-262.
53. A. N. Thadani, Y. Huang and V. H. Rawal, *Organic Letters*, 2007, **9**, 3873-3876.
54. S. Ay, M. Nieger and S. Brase, *Chemistry - A European Journal*, 2008, **14**, 11539-11556.
55. Compound (*R,R*)-**3** could not be purified on a large scale, however a small amount of pure material was isolated for characterization by NMR spectroscopy.
56. H. C. Chen and S. H. Chen, *Journal of Physical Chemistry*, 1984, **88**, 5118-5121.
57. M. Valentini, H. Ruegger and P. S. Pregosin, *Helvetica Chimica Acta*, 2001, **84**, 2833-2853.
58. C. M. Silvernail, L. J. Yao, L. M. R. Hill, M. A. Hillmyer and W. B. Tolman, *Inorganic Chemistry*, 2007, **46**, 6565-6574.
59. M. Gennari, M. Tegoni, M. Lanfranchi, M. A. Pellinghelli, M. Gianetto and L. Marchio, *Inorganic Chemistry*, 2008, **47**, 2223-2232.
60. A. Macchioni, G. Ciancaleoni, C. Zuccaccia and D. Zuccaccia, *Chemical Society Reviews*, 2008, **37**, 479-489.
61. J. F. Larrow, E. N. Jacobsen, Y. Gao, Y. P. Hong, X. Y. Nie and C. M. Zepp, *Journal of Organic Chemistry*, 1994, **59**, 1939-1942.



Functionalized diaminophenolates as ligands for dinuclear indium catalysts were investigated in the ring-opening polymerization of lactide. An increase in the steric bulk of the ligand phenolates decreases the selectivity of the catalysts due to catalyst dissociation during polymerization.